

Article

Archaeoseismological Evidence of Seismic Damage at Medina Azahara (Córdoba, Spain) from the Early 11th Century

Miguel Ángel Rodríguez-Pascua ^{1,*}, María Ángeles Perucha ¹, Pablo G. Silva ², Alberto Javier Montejo Córdoba ³, Jorge Luis Giner-Robles ⁴, Javier Élez ⁵, Teresa Bardají ⁶, Elvira Roquero ⁷ and Yolanda Sánchez-Sánchez ⁵

¹ Instituto Geológico y Minero de España (IGME-CSIC), Ríos Rosas 23, 28003 Madrid, Spain

² Departamento Geología, Escuela Politécnica Superior de Ávila, Universidad Salamanca, Hornos Caleros 50, 05003 Ávila, Spain

³ Consejería de Cultura y Patrimonio Histórico, Junta de Andalucía, Capitulares 2, 14002 Córdoba, Spain

⁴ Departamento Geología, Facultad de Ciencias, Universidad Autónoma de Madrid, Cantoblanco, 28049 Tres Cantos, Spain

⁵ Departamento Geología, Facultad de Ciencias, Universidad de Salamanca, Plaza de la Merced s/n, 37008 Salamanca, Spain

⁶ Departamento Geología, Geografía y Medio Ambiente, Facultad de Ciencias, Universidad de Alcalá, 28871 Alcalá de Henares, Spain

⁷ Departamento Edafología, ETSI Agrónomos, Universidad Politécnica de Madrid, 28040 Madrid, Spain

* Correspondence: ma.rodriguez@igme.es

Abstract: The “Caliphal City of Medina Azahara” was built in 936–937 CE or 940–941 CE (depending on the source) by the first Caliph of al-Andalus Abd al-Rahman III, being recently inscribed (2018) on the UNESCO World Heritage List. The abandonment and destruction of the city have been traditionally related to the civil war (“*fitna*”) that started between 1009 and 1010 CE. However, we cannot rule out other causes for the rapid depopulation and plundering of the city just a few decades after its foundation. The archaeoseismological study provides the first clues on the possible role played by an earthquake in the sudden abandonment and ruin of the city. Eleven different types of Earthquake Archaeological Effects (EAEs) have been identified, such as dropped key stones in arches, tilted walls, conjugated fractures in brick-made walls, conjugated fractures and folds in regular pavements and dipping broken corners in columns, among others. Besides that, 163 structural measures on EAEs were surveyed resulting in a mean ground movement direction of N140°–160° E. This geological structural analysis clearly indicates a building-oriented damage, which can be reasonably attributed to an earthquake that devastated Medina Azahara during the 11st or 12th centuries CE. If this were the case, two strong earthquakes (\geq VIII MSK/EMS) occurred in 1024–1025 CE and 1169–1170 CE could be the suspected causative events of the damage and destruction of the city.

Keywords: Medina Azahara; Earthquake Archaeological Effects (EAEs); geological structural analysis; city destruction and abandonment; South Spain



Citation: Rodríguez-Pascua, M.Á.; Perucha, M.Á.; Silva, P.G.; Montejo Córdoba, A.J.; Giner-Robles, J.L.; Élez, J.; Bardají, T.; Roquero, E.; Sánchez-Sánchez, Y.

Archaeoseismological Evidence of Seismic Damage at Medina Azahara (Córdoba, Spain) from the Early 11th Century. *Appl. Sci.* **2023**, *13*, 1601. <https://doi.org/10.3390/app13031601>

Academic Editor: Nicola Ruggieri

Received: 21 December 2022

Revised: 16 January 2023

Accepted: 17 January 2023

Published: 26 January 2023



Copyright: © 2023 by the authors. Licensee MDPI, Basel, Switzerland. This article is an open access article distributed under the terms and conditions of the Creative Commons Attribution (CC BY) license (<https://creativecommons.org/licenses/by/4.0/>).

1. Introduction

The causes that led to the destruction and abandonment of many archaeological sites are still subject of intense debate, especially when dealing with medieval or antiquity sites. Since the emergence of archaeoseismology, earthquakes are playing a heading role to explain the decadence, abandonment and destruction of many ancient sites around the Mediterranean Sea [1–3]. The present study deals with the premature abandonment and destruction of Medina Azahara, Capital of the Umayyad Caliphate of Cordoba (Andalusia, Spain) between the late 10th and the early 11th centuries. Medina Azahara, under the protection of the Andalusian Government, is included in the UNESCO World Heritage List since 2018 constituting one of the most important architectural masterpieces of the Al Andalus in the Iberian Peninsula.

The Caliphal city was founded between the years 935–941 CE, being the court of Abd al-Rahman III and its successor al-Hakan II till the years 975–977 CE [4,5]. After this time, the Andalusi military leader Almanzor took the power acting as the regent of the Caliphate [6]. A subsequent tumultuous period of upheavals and power struggles ended in a civil war (*fitna*) between the years 1009–1031 CE [4] and the final collapse of the Umayyad Caliphate in Al-Andalus. Along all this period, the luxury caliphal city was only active during around 40–45 years being abruptly abandoned soon after the death of Abd al-Rahman III. The sudden abandonment and decline of Medina Azahara are still under debate among the archaeological community since any ancient chronicle describes the city destruction or its subsequent plundering [4].

Interestingly, during the second half of the 10th century, there is a well-documented seismic period across the whole Al-Andalus, but especially around Cordoba [7–10]. In fact, this seismic period is the first historically documented one in the Iberian Peninsula by almost contemporary written chronicles. Recent revisions of historical seismic catalogues in Spain show that these earthquakes are well grounded by Arabic historians who gave accurate dates with the year, month, day and even the hour of the catalogued events [10–12]. This seismic period extends from the year 944 CE till 974 CE, overlapping the lifetime of the studied caliphal site (Appendix A), suddenly abandoned in the year 975 CE [5]. Other destructive, strong earthquakes occurred in the zone soon after this period in the years 986–987 CE (\geq VII MSK), 1024–125 CE (VIII–IX MSK) and 1169–1070 CE (IX–X MSK), could have contributed to the late ruin and destruction of the already abandoned site (see Appendix A; Figure 1). All these earthquakes are listed in the exiting on-line seismic catalogues of the Spanish Geological Survey [13], Instituto Andalúz de Geofísica [14] and the Instituto Geográfico Nacional [15]. Consequently, the occurrence of earthquake damage cannot be ruled out at all as a triggering factor (among others) of the sudden abandonment, destruction and late ruin of the caliphal city. In this work, we present the analysis of 163 earthquake archaeological effects (EAEs) surveyed within the site to check the probable seismic origin of the observed deformations by means of the study of oriented damage.

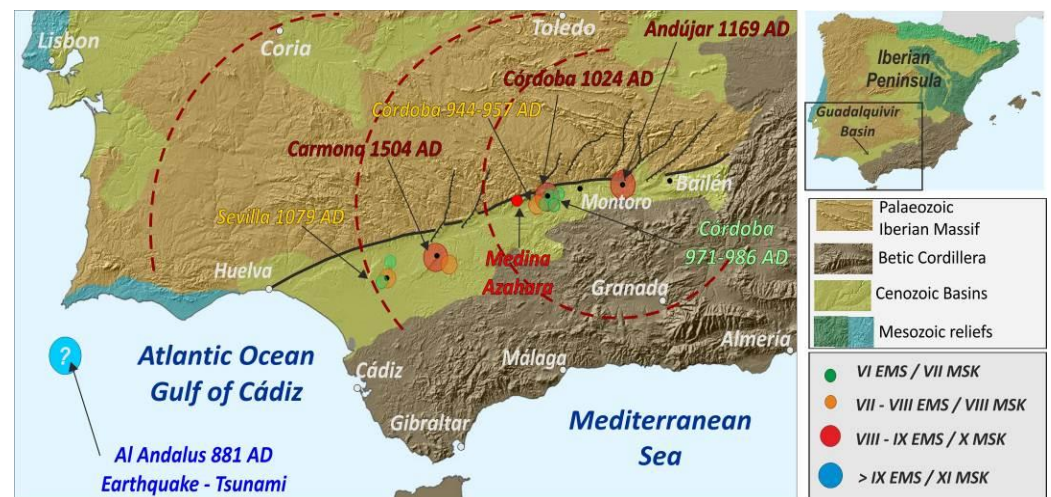


Figure 1. Geological setting of the Caliphal City of Medina Azahara in the framework of the Guadalquivir Basin (SW Spain). Main faults and macroseismic epicenters of the most important historical earthquakes occurred in Al-Andalus between the years 940 CE and 1504 CE are showed (see Appendix A for seismic details).

2. Geological and Geodynamic Setting

The ancient city of Medina Azahara is located in southern Spain (Andalusia), close to the city of Córdoba, on the boundary between the Paleozoic reliefs of Sierra Morena and the Neogene Guadalquivir sedimentary basin (Figure 1).

The Guadalquivir Neogene Basin corresponds to the foreland basin of the Betic Cordillera (Figure 1) and is filled by a thick sedimentary succession (c. 1.5 km) of Miocene to Pliocene marine deposits and olisthostromic units from the last c. 15.5 Ma [16]. To the south olisthostrome melange is imbricated and overridden by the proximal tectonic wedges formed by Triassic to Paleogene materials along the Betic thrust-front [17]. Tectonic loading along the Betic front and continuous sedimentation from 10.5 to 5.5 Ma caused significant lithospheric overloading triggering isostatic forebulging along the northern margin of the basin and the adjacent Paleozoic materials of the Iberian massif [17,18] (Figure 2A). Following these authors, Pliocene to Quaternary isostatic forebulging propagated to the North into the Iberian massif giving rise to flexural upfolding in the Paleozoic materials and relief generation (i.e., Sierra Morena). Upfolding also affected to the Miocene calcarenites along the northern margin of the Guadalquivir Depression facilitating its deformation and subaerial erosion. Nowadays, isolated patches of these eroded and uplifted Miocene materials lying unconformably on the metamorphic substratum provide evidence of the process (Figure 2B). Tectonic relief rejuvenation processes of the northern edge of the Guadalquivir basin have been described using geomorphological indexes and associated with the seismic activity of this fault [19–22]. As illustrated in Figure 1, NNE-SSW to nearly N-S normal faults segment the trace of the NE-SW border of the Guadalquivir Basin, a complex erosive-mechanical contact historically known as the “Great Betic Fault” or the Guadalquivir Fault Zone (GFZ) [21,22]. The GFZ is a large fault-flexure fragmented (split) in multiple subparallel inducing the bending and upfolding of the Paleozoic basement for about 1500 m beneath the central sector of the basin to the northern reliefs of Sierra Morena [23]. This tectonic flexure induced the uplift of Sierra Morena which marks the southern end of the Iberian Paleozoic plateau generating an important topographic step and the uplift of the overlying Late Neogene materials [24]. Cartographic and geophysical data indicate that the uplift of the late Neogene calcarenites within the Sierra Morena range reach up to 420–450 m for the last c.a. 5 M.a. [17,24]. This accumulated uplift will indicate uplift rates of about 0.09–0.1 mm/year, sufficient to explain the seismicity of the zone [17,22]. Crustal bending promoted and assisted brittle deformation at upper crustal levels (<30 km) resulting in NNE-SSW to NE-SW normal faulting in the backbulge zone [18,25] delineating the northern border of the basin (Figure 2). Following these authors, these normal faults are the responsible of the instrumental seismicity along the northern border of the Guadalquivir basin (Figure 2A), but buried reverse faulting is also responsible of the variety of seismic series and swarms instrumentally recorded in the southern zone of the basin since the early 20th century [18,25,26].

Research on the Andujar 1069–1970 CE [27] and Carmona 1504 CE historical earthquakes [21] also suggest that backbulge normal faulting along the NNE-SSW to NE-SW faults are the responsible sources of these historical events. Geological data indicate that these two strong earthquakes were no-surface faulting events with estimated magnitudes of 6.0 and 6.2 M_w , but with an important damage potential (\geq VII MSK) in 50–80 km radii [9,13].

In detail, as mapped in the 1:50,000 geological chart of the zone [28], Medina Azahara is just located on the trace of the mentioned Guadalquivir Fault Zone (GFZ), which comprises several subparallel minor faults stepping the Late Neogene sediments basin wards (Figure 2A). These faults are subvertical and affect to the gently dipping (10–15° SE) Late Miocene calcarenites and marls overlapping the Paleozoic materials of Sierra Morena (Figure 2B). Normal faulting affects the Paleozoic basement and Late Neogene materials across the northern margin of the basin but there are no surface faulting elements. For this reason, these faults are considered as late Neogene faults [28], but instrumental seismicity ($m_b < 4.5$) with normal faulting focal solutions is common along the northern margin of the basin [18,27] (Figure 2A). In the same way, important instrumental seismic swarms are recorded towards the southern margin of the basin, which are related to subsurface reverse faulting affecting the Paleozoic basement [18] (Figure 2A).

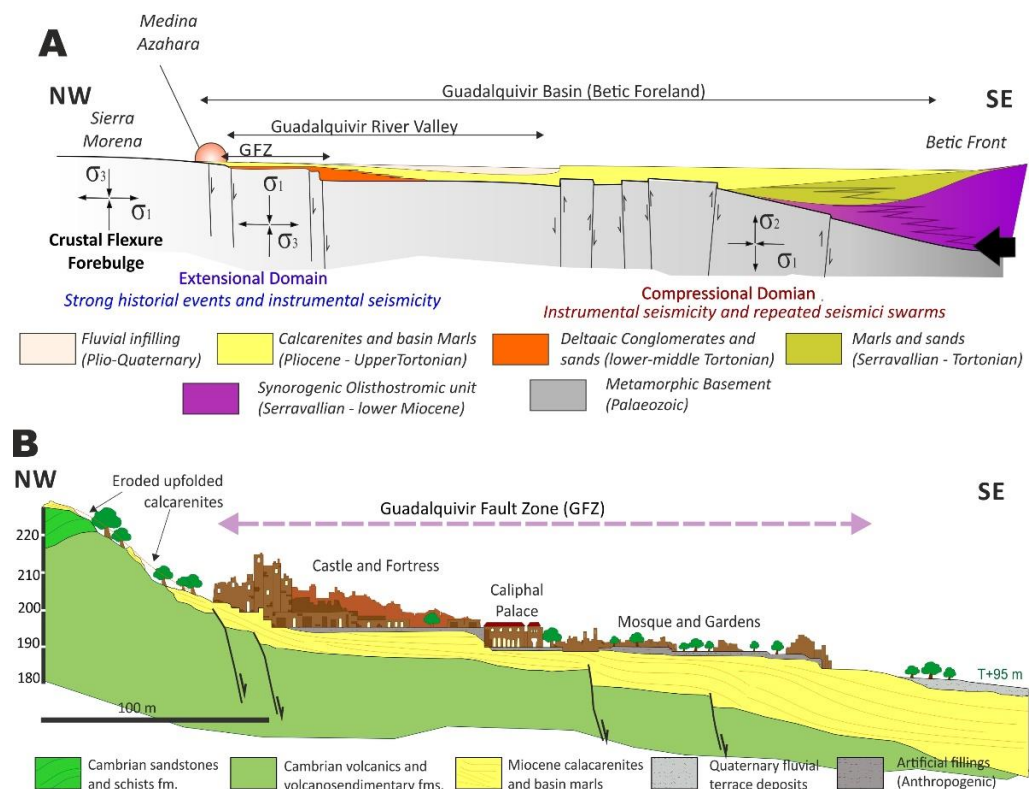


Figure 2. Geologic and Geodynamic setting of the Archaeological site of Medina Azahara. (A): General sketch showing the lithospheric structure of the Betic foreland basin, flexural processes and related seismicity. Based in data from [17,18] (not scaled). The cross-section displays the buried faults and stress tensors (σ_1 – σ_2 – σ_3) deduced for recent focal solutions related with ongoing flexural process throughout the basin in the northern zone of the basin [18] (B): Geological cross-section displaying the structural arrangement of Paleozoic and Cenozoic materials beneath Medina Azahara. Based in the geological map of the zone [28] Vertical Exaggeration $\times 4$.

Paleozoic materials in the area are mainly constituted by variably metamorphosed volcanic and volcanoclastic formations of the Lower Cambrian to Ordovician age [29,30]. Regarding the Neogene materials, they are littoral and marine sediments filling the sedimentary trough and overlapping the northern Paleozoic materials. In the studied zone, these are mainly biocalcarenes, algae limestones and interbedded sands and yellow silts [28]. The substratum of the area has an upper Tortonian to Messinian age, but to the south (Carmona–Sevilla) these facies reach a Late Pliocene age following the progressive filling of the foreland basin during the Late Neogene [16]. In detail, the Neogene biocalcarenes and limestones from local quarries were the main construction materials in Medina Azahara, although other Paleozoic lithologies such as marbles, schists, gabbros, granites and other valuable exotic rocks were also used [31]. Overlapping the Neogene materials outcrops, the extensive formation of Quaternary alluvial deposits of the Guadalquivir River develop (Figure 2).

3. Historical and Instrumental Seismicity in the Guadalquivir Basin

Seismicity is not an outstanding process within the Guadalquivir Depression, however, important historical destructive events (\geq VIII EMS) have occurred in the zone along the northern border of the Neogene basin (Figure 1; Appendix A). In detail, aside from those events that occurred during the Islamic period, the city of Córdoba was the subject of an important seismic sequence during the late 19th century (1863–1900). During this modern seismic period, maximum estimated intensities reached up to VI EMS [15] (IGN, 2022). Contrastingly, instrumental seismicity is not relevant (<4.0 mb; \leq V EMS) and it is mostly related to seismic series that occurred along the northern border of the basin between the

year 1945 and the present day [15]. However, more persistent and moderate instrumental seismicity (<4.5 mb; \leq VI EMS) is recorded along the southern Betic front of the basin [25,26]. These southern events are mainly seismic swarms related to blind reverse and strike-slip faults within the basin [18,25]. Figure 2A illustrate the location and kinematics of the northern and southern buried faults of the Guadalquivir basin in relation to the isostatic flexure of the zone, as proposed by some authors [18].

Regarding to historical seismicity, the more important events occurred during the lifetime of the caliphal city or soon after its abandonment, that is, during the second half of the 10th century and from 11th to 12th centuries (Appendix A). Figure 3 illustrates the different historical seismic periods and events in relation to the construction, rise and fall of Medina Azahara.

Two seismic periods between the years 944–957 CE (\leq VII MSK) and 971–974 CE (\leq VI–VII MSK), overlap the lifetime of the caliphal city (Appendix A; Figure 3). The last period occurred just before its sudden abandonment in the year 975 CE [5] (Figure 3) and the last event (974 CE) was strong enough to be felt in Extremadura (Coria) and Toledo about 300 km away [9]. Historical accounts on this earthquake describe: “On Monday 21st of Safar (Year of the Hijra 364 = 9 November, 974 CE), at the end of the midday prayer, an earthquake happened in Cordoba and its surrounding region, well perceived but of short duration. The tremor was felt at the same time in all the Andalusi regions. The police chief and military governor of the Jawf (Extremadura and its adjacent parts), Ya’la b. Ahmad, wrote from the city of Coria reporting on this earthquake, as well as the exact date and hour of the event [32].

These two groups of earthquakes are well grounded on accounts by Arabic historians, with descriptions of slight building damage in Cordoba, especially those of the first seismic period [9,10,32]. However, these earthquakes do not seem to have sufficient destructive potential to promote the abandonment of the studied site, but maybe to cause some deformations and minor EAEs. However, other destructive earthquakes occurred in the zone after this period in the years 986–987 CE (\geq VII MSK), 1024 CE (VIII–IX MSK) and 1169 CE (IX–X MSK), strong enough to produce noticeable to important damage in the studied site (Appendix A; Figure 3). The first event occurred in Cordoba, damaging one of the bridges of the city [33], and the two others affected the territory of the Cordoba Caliphate to a different extent [9].

The 1024–1025 CE (VIII–IX MSK) event is known as the Great Al-Andalus Earthquake, but available descriptions are rather vague enough to locate the earthquake. The only written description says: “In the year of the Hijra 415 (15 March 1024–30 March 1025) a great earthquake occurred in al-Andalus. Mountains collapsed, the earth was shattered, and buildings were destroyed by the violence of the tremor” [32]. The Earthquake was dated on 15 March 1024 [9,10], was felt in Almería and in most of the territory of the Umayyad Caliphate, including Córdoba. Ref. [8] assign to this earthquake an intensity VIII–IX MSK (Appendix A), but its precise location needs of more historical or geological records [10,34]. This earthquake is not listed in contemporary Arab reports and it is only cited in the manuscript *Rawḍ al-Qirṭās*, a chronicle of the history of Morocco kingdom written in the early 14th century, the reason for which is considered by some authors as a doubtful event [10]. Whatever the case, it is still listed in historical catalogues for Spain and the Mediterranean region [10,14]. Additionally, the zone was affected by a moderate earthquake in 1079–1080 CE (\geq VI; Appendix A) which shook the entire region of Al-Andalus causing damage in Sevilla and affecting La Giralda (Minaret of the main mosque of the city), which had to be repaired, leaving epigraphic evidence [10,14,34].

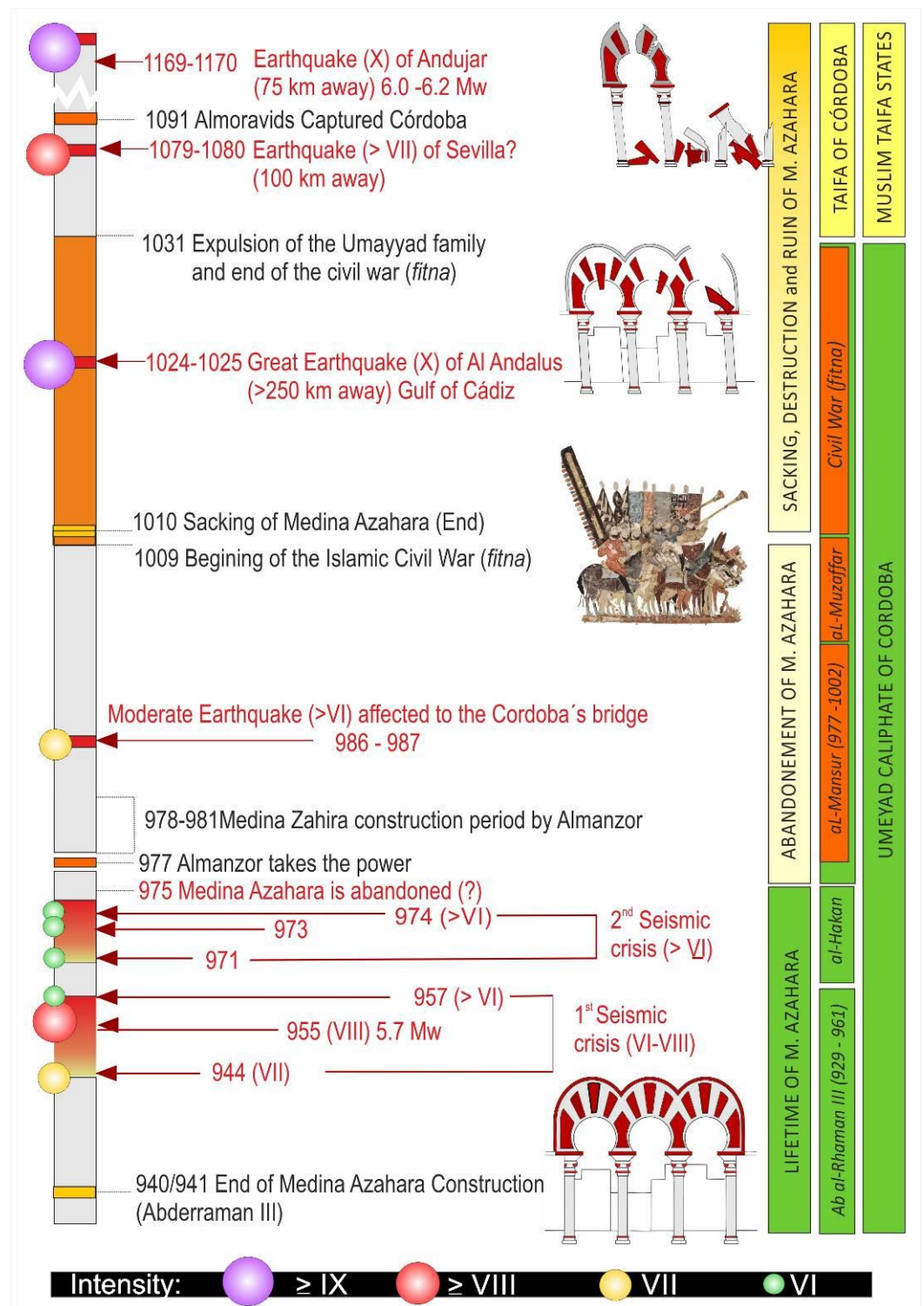


Figure 3. Composite graphic timeline of most important historical success and seismic events occurred during the construction, lifetime, abandonment, destruction and ruin of the Caliphal city of Medina Azahara (944–1169 CE).

On the contrary the 1169–1170 CE event (IX-X MSK) is well reported in contemporary chronicles and latter historical reports [9,10,34]. This is the so-called Andujar Earthquake (c. 60 km away) which affected the localities of Cordoba and Granada (VII MSK), Sevilla (VI MSK), Toledo (III MSK), and was felt in distant localities of Extremadura and Almería about 350 km away [10,15,27] (Figure 1). This was a large earthquake that produced important

environmental effects within the Guadalquivir valley [13,27]. The contemporary records indicate: *“In the year 565 of the Hijra (1169–1170 CE) a great earthquake occurred between the sunrise and sunset during the first Jumada (January–February 1170) in part of the region of al-Andalus; the people observed how the walls move and bend towards the ground but then they became straight again and recovered their original state by the benevolence of Allah. Many houses and the minarets of the cities of Cordoba, Granada and Seville were damaged and collapsed. The place of Andujar was the most damaged site, since in that site tremors lasted for several days until the village almost disappeared lost under the earth.”* English translation of original transcriptions in [32,34].

Among other contemporary chronicles, it is worthy to note that of the Arabic cordovan philosopher “Averroes” (1126–1190 CE) wrote in its book “Talkhis al-athar” (pages 130–131): *“I was not then in Cordoba during the earthquake occurred in the year 565 (1169–1170 CE), but I arrived shortly after, and I could hear the sounds that occur after the earthquakes. People thought that the noise came from the West, and I considered that earthquakes are often triggered by the formation of westerly winds. (. . .) Strong earthquakes affected Cordoba for a year, and tremors only stopped three years later. The first earthquake killed many people in Cordoba by the collapse of buildings. It was said that the ground cracked near this city, in the place called Andujar, where something like dirt or sand poured from the cracks (e.g., liquefaction). (. . .) The earthquakes extended throughout the Western part of the Peninsula, but especially affected Cordoba and its region. The earthquakes were felt stronger in the east of the city than in the city itself and were weaker in the west than in the city. (. . .) The earthquake was stronger in Andujar than at any other point. The people of Jerez, near Seville, said that on the days of the earthquakes heavy vapors emerged from the ground dense enough to prevented sight.”* English translation of original transcriptions in [25,27,35].

This historically documented event triggered important building damage and fatalities in Cordoba (\geq VIII MSK/EMS), ground cracking and liquefaction processes throughout the Guadalquivir valley [13], as well as archaeoseismic damage in Andujar [27]. Historical descriptions from “Averroes” indicate that tremors came from the west of Córdoba, where is located the basin boundary (GFZ), but also that ground shaking was weaker in the Paleozoic reliefs (west) than in the softer river valley alluvium east to the city. In summary, this was an important event with an estimated magnitude of c. 6.0 Mw part and beginning of a seismic sequence that lasted at least three years [10,27,34]. Therefore, this strong event might really contribute to the damage and destruction of Medina Azahara, probably in a ruin state after its abandonment (Figure 3). Maybe this is also the case of the 1024–1025 CE Great Al-Andalus Earthquake, but available descriptions do not allow either more precise interpretations (Appendix A) or the identification of the responsible seismic sources of these historical events [13]. After the Andujar earthquake, the following notable event occurred in the zone was in the year 1504, severely damaging the City of Carmona (X MSK), about 100 km away SW from Córdoba (Appendix A; Figure 1). All the aforementioned studies of these historical earthquakes suggest that brittle deformation along the complex mechanical contact bounding the northern margin of the basin (GDF; Figures 1 and 2) could work as a reliable seismic source [21,27].

4. Historical Setting

Medina Azahara was built by the first Umayyad Caliph of al-Andalus, Abd al-Rahmān III (912–961 CE) in the year 329 of the Hijra, which corresponds to 936–937 CE or 940–941 CE (depending on the written sources). This city is located about 6 km west of Cordoba, close to the foothills of Sierra Morena at the piedmont of the Guadalquivir valley (Figures 1 and 2). The urban zone expanded over an area of about 115 Ha, with only 10% excavated up to now [5]. The city was the official residence of the court and of different government units such as the Ceca (The Mint). The importance of this city is evidenced by the exuberant decoration and quality of its buildings (marbles, copper, silver, etc.), such as the Abd al-Rahmān III Saloon, the Great Portico or the Gardens. The Caliph al-Hakam II (961–976 CE), continued the construction and adornment of Medina Azahara, initiated by his father. This

second Caliph was succeeded by his young son Hisam II (11 years old) in 976 CE who reigned until the expulsion of the Umayyad family from Al-Andalus in 1013 CE (Figure 3).

Despite the monumentality and richness of Medina Azahara, the city had a very short life of only 35 years. One of the reasons of the rapid decline of the city could be the designation of the chancellor “Almanzor” (Al-Mansur) as chamberlain (hajib) of the young caliph in 977 CE, imposing important changes in the policies of the Islamic Iberia [6]. In 978–979 CE, Almanzor began the construction of a new Caliphal city (Medina Alazhira) east of Córdoba close to the Guadalquivir River, just in the opposite direction of Medina Azahara (Figure 3). This new city was finished in 980–981 CE, becoming the site of the new administrative centre and residence of the caliphate. This caused the sudden disuse, progressive oblivion and abandonment of Medina Azahara. The absence of epigraphic records in Medina Azahara regarding to new building improvements in the name of Hisam II (third and last Umayyad Caliph) evidence this change in the capital status of the city [36]. During this period, Almanzor was in fact the ruler of Islamic Iberia giving place to numerous fights of power between the Umayyad family, Almanzor and its heirs (sons and grandsons). These continuous political disturbances led to the insurrection of the population, the capture of the Alcázar of Cordoba, the execution of the Almanzor’s son/heir and military overthrows of African Berber troops during 1009 CE. Eventually, the insurgence led to a violent civil war (*fitna*) that terminated with the Umayyad Caliphate in the Islamic Iberia between 1009 and 1031 CE (Figure 3), but also with the assault, looting and partial destruction of both Medina Azahara and Medina Alzahira [4]. Medina Alzahira (Almanzor palace), raided on February 1009 CE suffered such a level of destruction to the extent that it has not been certainly located to date [4]. On the contrary, historical accounts only refer to the assault and looting of Medina Azahara in June 1010 CE by Berber Troops, but no written records mention to its destruction [5]. The historical chronicles refer to the “plundering of wealth” of Medina Azahara indicating that the “African crowds raided tapestries, lanterns, doors and Qur’ans of the main mosque” and probably also rushed other areas of the city [4].

Whatever the case, the civil war (*fitna*) is the most widely accepted hypothesis for the abrupt abandonment and destruction of the studied caliphal city, and the year 1010 CE is conventionally established as the end of its lifetime among the archaeological community [5]. However, the “*fitna*” continued till the end of 1031 CE and almost 21 years (1010–1031 CE) of history in Medina Azahara are not documented [4]. After the end of the “*fitna*”, the abandoned city was gradually raided by the Almoravids and Almohads (later Taifa kingdoms), and most of the expensive construction materials, (e.g., ashlars, capitals, drums, marbles, etc.) and metals (e.g., copper from doors, lead from pipes, etc.) were removed, stolen and reused for building new Arabic palaces and mosques in Sevilla, Granada, Tarragona and even Marrakesh (Morocco). For instance, at the Alcazar and Giralda of Sevilla, there are dozens of capitals with dates and praises referring to the Cordovan Umayyads. Later on, when the Spanish Christian kingdoms recovered Córdoba, (1236 CE) the ancient Medina Azahara, so-called “Córdoba La Vieja” (Old Cordoba), was already ruined and partially buried by talus deposits. Even in this stage, the ruins were used as quarry for the construction of churches and monasteries around Córdoba. Before the first archaeological excavations during the early 20th century (1911 CE) most of the ruins, especially their lower southern sectors, were practically buried by thick talus-slope deposits [5,37].

In this study we analyze the probable contribution of seismic activity in the decadence and ruin of Medina Azahara. As aforementioned, the late 10th century CE and the following 11th and 12th centuries were an intense seismic period around Cordoba with moderate earthquakes before its early abandonment in the year 975 CE, and strong later earthquakes (\geq VIII EMS) in the years 1024–125, 1079–1080 and 1169–1170 CE (Appendix A; Figure 3). The cornerstone of the performed analysis is to be capable to correlate some of the catalogued earthquakes and the date of collapse, destruction, or ruin of different buildings or structures within Medina Azahara. In this way, it is necessary to identify

whether the collapses took place before or after 1009 CE, starting date of the civil war (*fitna*) that led to the end of the Umayyad Caliphate (Figure 3), but also if the documented damage could occur afterwards during the later strong earthquakes. However, this is a difficult goal to achieve since archaeological excavations, multiple restorations and reconstructions carried out in the studied site since the early 20th century are randomly documented from the stratigraphic point of view [5].

5. Methodology

Despite the existence of different approaches on archaeoseismological research, e.g., [2,38–45], the present study follows the guidelines of the oriented damage analysis in Earthquake Archaeological Effects (EAEs) by means of structural geology practices [41,44,45]. The studied site does not have the essential stratigraphic and tectonic characteristics to apply the most classical archaeoseismic geoarchaeological methodology [2], such as the analysis of fresh cut-slopes, modern excavations or close fault surface ruptures. On the contrary, the site has been excavated since the early 20th century and an important graphic documentary research (analysis of old photos, drawings, maps, etc.) has been necessary to explore old excavations, cut-slopes and discriminate reconstructions or restorations to identify and validate the studied deformations (EAEs). The performed analysis applies the geological structural analysis of deformed elements in pavements, walls, arches, etc., to recognize a probable oriented damage (i.e., seismic origin) of the EAEs presently recorded in the archaeological site. In detail, some of the EAEs preserve sufficient elements to apply the field or mathematical approaches to unravel past ground motion, i.e., [38,39], but most of them allow for the structural geology techniques by multiple compass measurements [43–45].

All the studied deformations are within the existing EAEs classification [41], and therefore subject to the proposed geological analyses. Eleven (11) different types of EAEs have been identified in this study: Collapsed key stones in arches (CKY), dropped key stones (DKY), directionally displaced columns (DDC), Block Extrusions in Walls (BEX), impact block marks (IBM), deformed and displaced vaults (DDV), tilted or folded walls (TFL), conjugated fractures in bricks-made walls (XFW), conjugated fractures on regular pavements (XFP), folds on regular pavements (FPV) and dipping broken corners in columns (DBC). These are distributed in 11 different sectors or buildings (Figure 4) and complete a dataset of 163 measured EAEs.

The collected structural data were catalogued and classified following the existing EAEs classification [41] and grouped in homogeneous datasets for the each one 13 of the studied sectors or buildings. Each dataset was later analyzed by means of the structural geological analysis to obtain the maximum deformation orientations (ey structural strain data) and generate a rose diagram for each analyzed sector or building (ey structural strain orientation) [43–45]. This analysis of strain structures results in the maximum strain horizontal direction of the ground (e.g., SHmax) for each site and allows for identifying the occurrence (or not) of building oriented damage (BOD) [44,45]. Once all the strain datasets defined by different EAEs within the studied site have been obtained, we proceed to plot the direction of SHmax trajectories on the map of the archaeological site. The obtained SHmax trajectories across the site can then be related to the mean direction of ground motion (oscillatory movement of the ground) generated by an earthquake, as checked for some ancient earthquakes (i.e., *Baelo Claudia*) [40,42], but also proved for instrumental events [44,45].

If the obtained strain orientation dataset (BOD) displays homogeneous trajectories with consistent overall orientation across a site, then seismic damage is feasible, since the damage may appear oriented in relation to the focal parameters of the causative earthquake as checked in instrumental events [43,46,47]. On the contrary, randomly or radially oriented strain data are normally indicative of a no seismic origin, and the concurrence of multiple processes in the deformation, destruction or ruin of a site can be addressed (e.g., explosions, assaults, etc., during a war: the *“fitna”* in our case) [41]. In these analyses, the concurrence

of different types of EAEs on walls, pavements, arches, columns, etc., indicating consistent orientations of ground motion reinforce the probable seismic origin of deformations [44,45]. However, it must not be forgotten that other factors can influence in the homogeneity of damage orientation, such as the urban pattern of the site (consistent orientation of streets and buildings), the slope of the site, the occurrence of slope processes, flooding, etc. [41] (e.g., 2, 3).

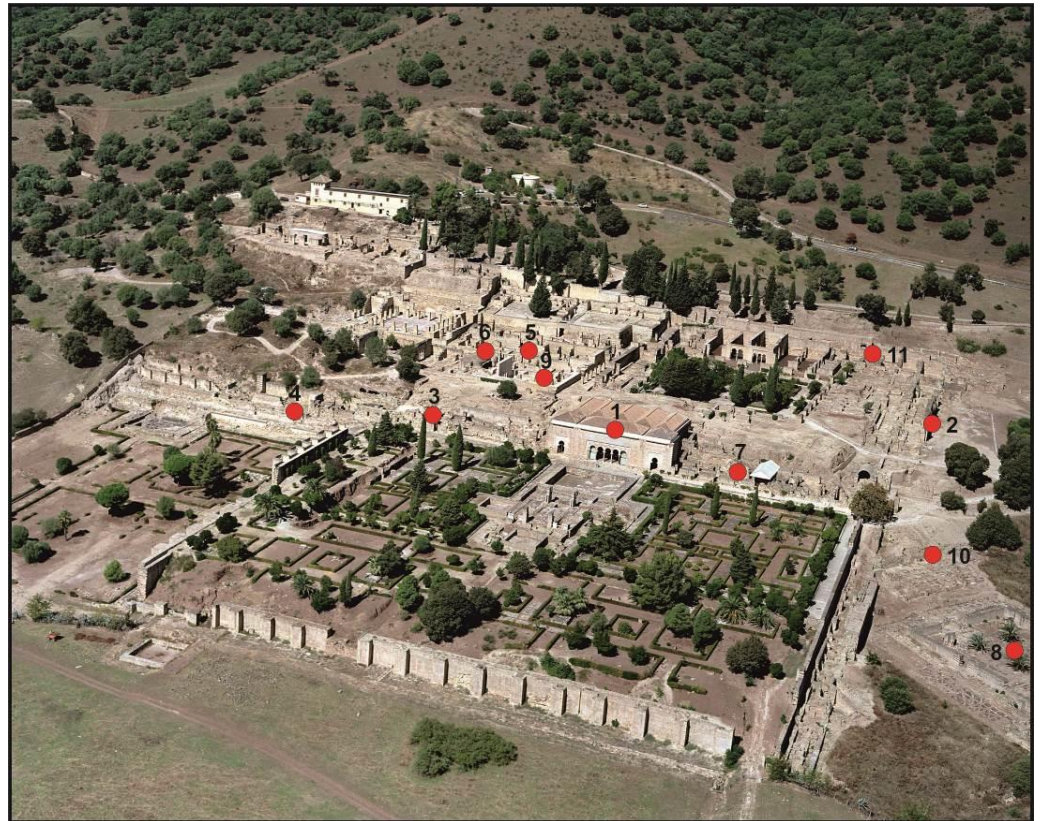


Figure 4. Aerial view of the archaeological site of Medina Azahara. The red dots are the location of the measurement of strain structures: 1—Abderraman III Saloon; 2—Porticos Entrance; 3—Ronda Way (Patrol Path); 4—Sewer of the patrol path; 5—The Oriental Service House (Oven); 6—Corridor of the Alberca House; 7—Attached Rooms to the Abderraman III Saloon; 8—Mosque; 9—Ya’far House; 10—Houses in the front of the Mosque; 11—defensive wall.

In summary, the methodological approach used in this study can be synthesized on the following five points:

1. Collection of data on deformation orientations in buildings at the archaeological site.
2. Cataloguing, classification and grouping (sectors or buildings) the measured deformation structures.
3. Geological structural analysis of the classified strain data to obtain individual strain data and mean/preferment directions of maximum horizontal strain (SHmax) for each one of the studied sectors or buildings.
4. Mapping and joint analysis of the resulting average SHmax trajectories to explore relationships with existent or suspect active tectonic structures in the area (if the case) to infer probable seismic sources.
5. Geoarchaeological checking of existent imagery material for 20th excavations to assess the most probable age of the studied deformations, collapses or displacements. In our case it is important to assess if those deformations occurred after, during or before the “*fitna*” (1009–1031 CE).

6. Archaeoseismological Evidences

EAEs can be classified into two major groups [41]: coseismic and post-seismic effects. In general, post-seismic effects are usually those that primarily imply that a given archaeological site may have been affected by an earthquake. One of these post-seismic effects is the unjustified abrupt abandonment of cities and settlements [1–3,41]. This is the case of the magnificent and luxurious city of Medina Azahara, which was abandoned without justification between 1009 and 1010 CE, after less than 35 years of occupation and activity. The “*fitna*” (1009–1031 CE) overlapped this period and is traditionally considered as the cause of the ruin of Medina Azahara [4,5], since historical accounts talk about violent assaults, robbery and destruction around the city of Cordoba (see Section 3). However, during the late 10th century and the years after the “*fitna*”, significant earthquakes also affected this zone (Appendix A; Figure 3) and seismic damage can be considered as one of the causes for the ruin and the sudden abandonment of the site. However, all the previous archaeological research of this site never considered this possibility.

During the field survey carried out in the archaeological site, 163 strain data were collected. Eleven (11) different types of EAEs were identified and measured (see Section 5) distributed in thirteen (13) different sectors or buildings (Figure 4). The catalogued EAEs are listed in Table 1 and described below indicating the results of the geological structural analysis for each case.

Table 1. Types and number of Earthquake Archaeological effects (EAEs) identified and measured in the Medina Azahara archaeological site classified in the different studied sectors or buildings of the ancient city. For location see Figure 4. Legend: Collapsed key stones in arches (CKY), dropped key stones (DKY), directionally displaced columns (DDC), Block Extrusions in Walls (BEX), impact block marks (IBM), deformed and displaced vaults (DDV), tilted or folded walls (TFL), conjugated fractures in bricks-made walls (XFW), conjugated fractures on regular pavements (XFP), folds on regular pavements (FPV) and dipping broken corners in columns (DBC).

Sector/Building	EAE Type	Measured Number	Mean Orientation
1. Salon Rico Abderraman III	DKY, DDC, DBC, XFP	36	N160° E to N-S
2. Porticos Entry Gates	CKY	3	N160° E
3. Ronda (Patrol Path)	DKY	2	N160° E to N-S
4. Sewer of Patrol Path	BEX	2	N-S
5. Oriental House (Ovens)	DDV, TWL	4	N145° E
6. Corridor Alberca House	TFL	32	N150° E
7. Rooms Abderraman III Saloon	XFP, IBM	16	N16°5 E
8. Main Mosque	XFP, IBM	59	N145° E
9. Ya’far House	IBM	2	inconclusive
10. Mosque Houses	FPV, IBM	3	N145° E
11. Northern defensive wall	TFL	1	N163° E

6.1. Collapsed and Dropped Keystones in Arches (CKY; DKY)

The fall or collapse of the keystones is a very common deformation generated during earthquakes [38,40,48] in arches from walls that are parallel to the seismic ray (direction of the seismic wave propagation). In some cases, the fall of the keystone can cause the complete collapse of the arches, and these collapses are clearly identifiable since they are parallel to the walls containing them. Arches perpendicular to the seismic wave arrival direction can collapse by tilting or they can present horizontal displacements of their keystones, instead of collapse [44]. In Medina Azahara, both phenomena, dropped and horizontally displaced keystones, have been documented (Figures 5–7).

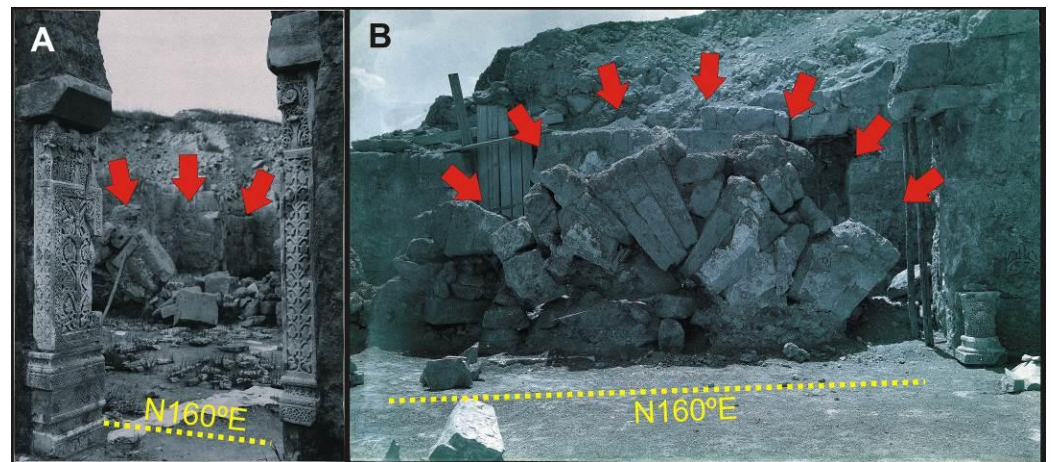


Figure 5. In situ collapsed arches in the Abderraman III Saloon. (A,B) interpretational sketches over the original photos from the excavations of the archaeologist Felix Hernández in 1943 (unpublished photographs). Red arrows indicate the collapsed and dropped keystones.



Figure 6. Collapsed arches in the Portico Zone: (A) General view of the arches, the yellow arrows mark the location of the collapsed arches in situ; (B) Collapsed arch marked like “B” in the (A) sketch; (C) Collapsed arch marked like “C” in the (A) sketch; (D) Collapsed arch marked like “D” in the (A) sketch.

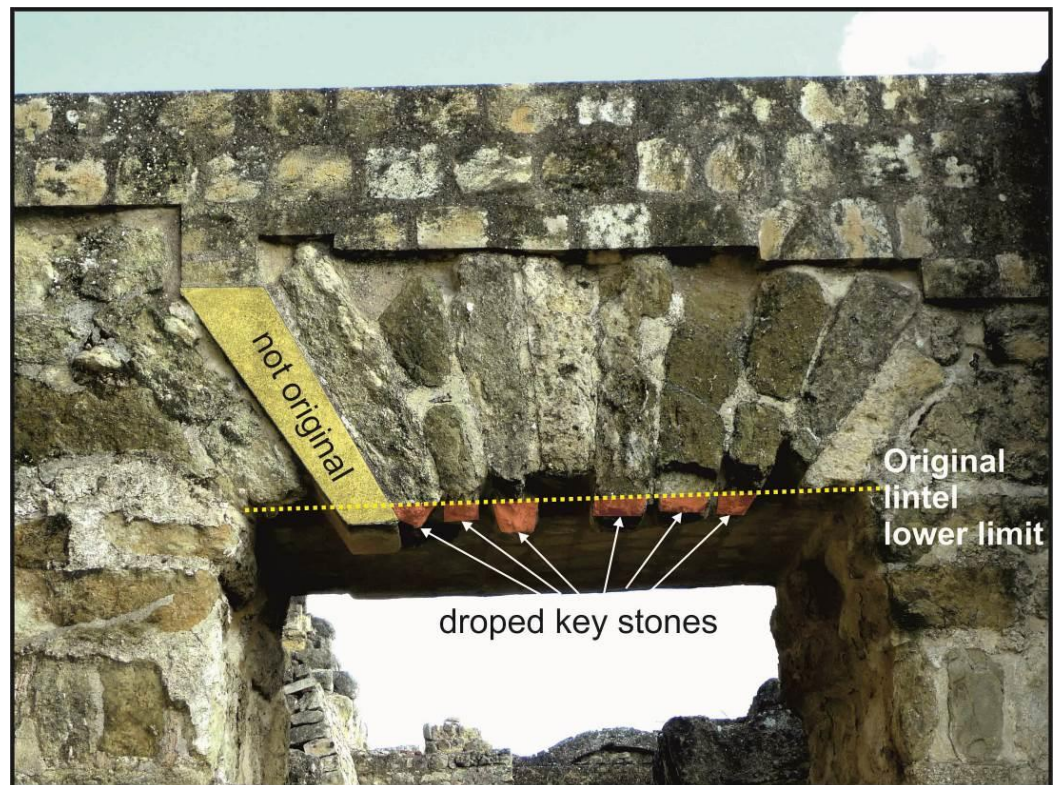


Figure 7. Dropped key stones in the Ronda Way zone. The direction of the wall that contain the arch is $N160^\circ E$.

Most of the original information from Medina Azahara has been lost, mainly because its ruins were quarried for centuries, but also because former archaeological methods of excavation were more extractive than conservative. However, we have been able to analyse some photographs from the early excavations (beginning of the 20th century) and recover some of this lost information. Two photographs of the Abderraman III Saloon (Figure 5) from the excavations carried out by the archaeologist Félix Hernández in the year 1943 [5] show collapsed arches clearly parallel to the walls that contained them, in a $N160^\circ E$ direction.

The same feature can be observed in the site called “Los Pórticos” (Figures 4 and 6), where three in situ collapsed arches present the same $N160^\circ E$ orientation (Figure 6B,C) as in the Abderraman III Saloon. The southernmost arch (Figure 6D) shows a dextraltwist in the sequence of key stones generated after the collapse, which could have been produced by the proper fall down of the arch or by a movement relative movement of the ground in NW-SE direction.

Both dropped (Figure 7) and horizontally displaced (Figure 8) keystones are also recorded in the site. They are located at the end of the patrol path and in one of the sewers drains of the lower garden area (Figure 4). In the first case, the direction of the movement needed to generate the fall of the keystone should be $N163^\circ E$ (Figure 7), compatible with the direction of horizontal movement of the drainage arch (Figure 8). This horizontal displacement even extruded up to 10–12 cm the mortar joining these arch keystones, showing also horizontal striations generated by the movement of the key (Figure 8B). This is a very good example of how two arches, perpendicular each other, behave under a same directional seismic shacking triggered by surface waves, giving in both cases the same average direction of ground movement.

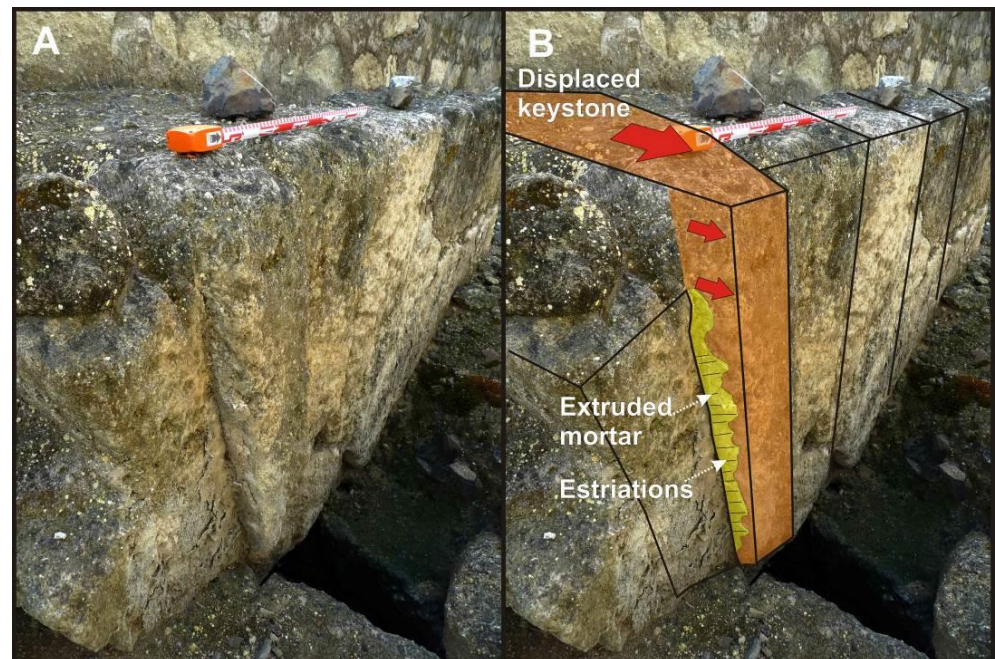


Figure 8. Horizontal displacement of key stones in a sewer at the Patrol Path zone: (A) perspective of the displaced key stone; (B) interpretative sketch, the displaced key stone is painted in orange (red arrow marks the direction of movement) and the yellow zone represents the extruded mortar from its original position.

6.2. Impact Block Marks (IBM)

The impact marks can indicate the direction and sense of the collapse of architectural elements that impact the pavements generating radial fractures [40,43,44,49]. This type of deformations can be observed around the Ya'far House (Figure 4) with regular marble pavement (Figure 9A) and in the Mosque with terracotta flagstones (Figure 9B). Unfortunately, the absence of the architectural elements that impacted the paved areas does not allow to determine the direction and sense of collapse. For this reason, these impact marks have been documented but cannot be used for geological structural analysis.

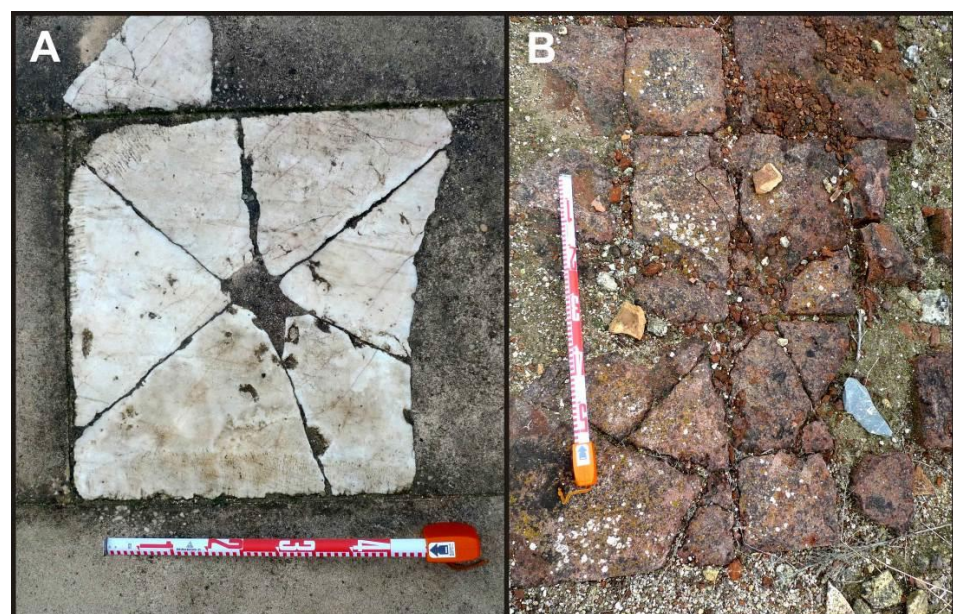


Figure 9. Impact marks: (A) Marble flagstone in the Ya'far House; (B) Terracotta flagstone in the Mosque.

6.3. Deformed and Displaced Vaults (DDV)

A very common EAE that affect the cultural heritage during earthquakes is the deformation, and eventual collapse, of vaults [50]. For example, the 2011 Lorca earthquake (Spain) generated a horizontal fracture with a 10–15 cm long displacement in the cross vault of the San Francisco Church coinciding with the direction of the arrival of surface seismic waves [49]. In Medina Azahara, the only preserved vaults are those of kitchen ovens, as the one preserved in the Eastern service house (Figures 4 and 10). The upper half of the brick vault of this oven is noticeably affected by a 10 to 16 cm horizontal displacement towards N135° E, making the structure too unstable to remove the archaeological filling of the oven to prevent its collapse (Figure 10A). As illustrated in Figure 10B, during seismic shaking, the circular ground base of the oven rotated in a counter-clockwise sense (towards the SE), triggering the visible twist of the oven vault. These kinds of rotations in circular elements without anisotropy, as orthogonal walls could be, are indicative of permanent ground deformation since the base of the structure rotates, but not its upper part [1,2]. Therefore, this EAE is an excellent indicator of the direction of maximum horizontal deformation (i.e., SHmax trajectories) [44,45].



Figure 10. (A) Deformed oven in the Oriental Service House and (B) interpretative sketch of the deformation structures (displaced vault). Arrows show the relative sense of rotation of the own elements.

6.4. Tilted Folded and Collapsed Walls (TFL)

This EAE is one of the most common effects observed in any urban area after an earthquake [44,51]. Tilted walls can be seen in photographs from former excavations, such as those carried out during the period 1992–1997 in this site [52]. These tilted walls were restored after the excavations, so we can only study them by using the old photographs (Figure 11). The best example of tilted wall is in the sector of the service houses (Figure 11A), where the main walls are tilted 9 degrees towards N160° E. On the other hand, oriented collapsed walls were excavated in several houses in front of the Mosque [37], where the collapse followed a N145° E direction (Figure 11B).

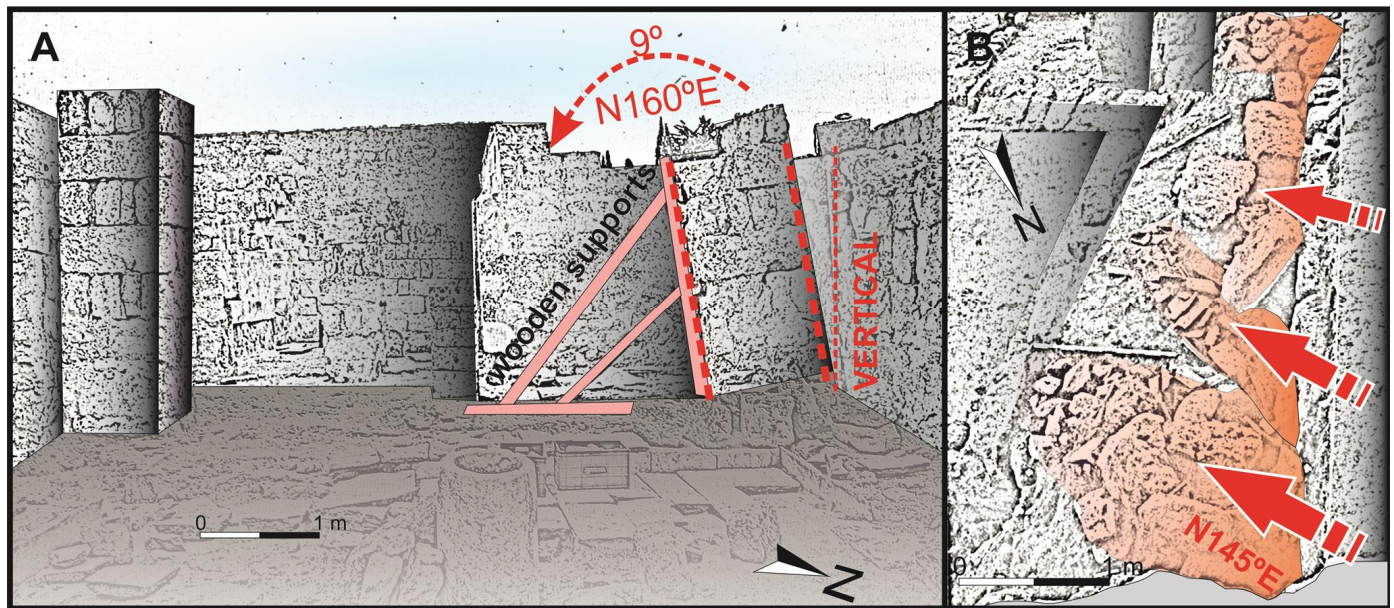


Figure 11. Tilted and collapsed walls: (A) tilted walls in the sector of the service houses. Photograph taken during the excavations of 1992–1997 (schematic shecht based on [52]) (B) collapsed walls in the houses in front of the Mosque (schematic shecht based on [37]).

6.5. Conjugated Fractures in Brick-Made Walls (XFW)

Cyclic shear movements generated by earthquakes in walls that are parallel to the direction of ground motion can generate conjugate fractures (X-fractures), which are a very common seismic effect in buildings deformed by earthquakes [43,44,50,53]. In Medina Azahara, most walls are masonry walls made up with blocks of carbonate sandstone (calcarenites) with different weathering degree that makes it very difficult to discern whether fractures were generated by an earthquake, or they were inherited from the original rock. In many cases, all traces of possible seismic deformation structures such as fractures (XFP) or dipping broken corners (DBC), have been erased by the weathering of the walls. However, conjugated fractures have been observed in the better-preserved brick walls, with the most interesting case in the corridor of the Alberca House (Figure 4).

The wall in this corridor is essentially made up of bricks with a mixed base of bricks and masonry blocks. Although this wall is affected by conjugated fractures, the most interesting phenomena is the development of “micro-fractures” in the bricks that behave fragile to deformation, while the mortar that joins them has a ductile-fragile behavior, which allows some inter-brick displacement. The horizontal movement of masonry blocks at the base of the walls by the cyclic shearing generated during seismic shaking, produce a compressive effect on the bricks beside and on the top of them (Figure 12A). Horizontal thrusting causes folding of the upper wall zone, generating compressional fractures (reverse faults) in the lower part and extensional fractures (normal faults) in the upper part (Figure 12B). A total of 6 reverse faults and 24 normal faults have been measured, congruent with a single horizontal shortening direction N155° E (Figure 12C). This phenomenon is common in the development of folds, where this type of deformation, compression in the lower part and extension in the upper part, is separated by the finite neutral surface (Figure 13). Conjugated compressive fractures follow Anderson’s classical fracture models, while extensional features follow the Slip Model [54]. In both cases, the three deformation axes remain parallel to each other, exchanging the axis of maximum shortening from the horizontal, in the case of compressional stresses, and to the vertical in the case of extensional ones, thus being a coaxial deformation compatible with a unique direction of maximum horizontal shortening (SHmax), N155° E in the studied case (Figure 13).

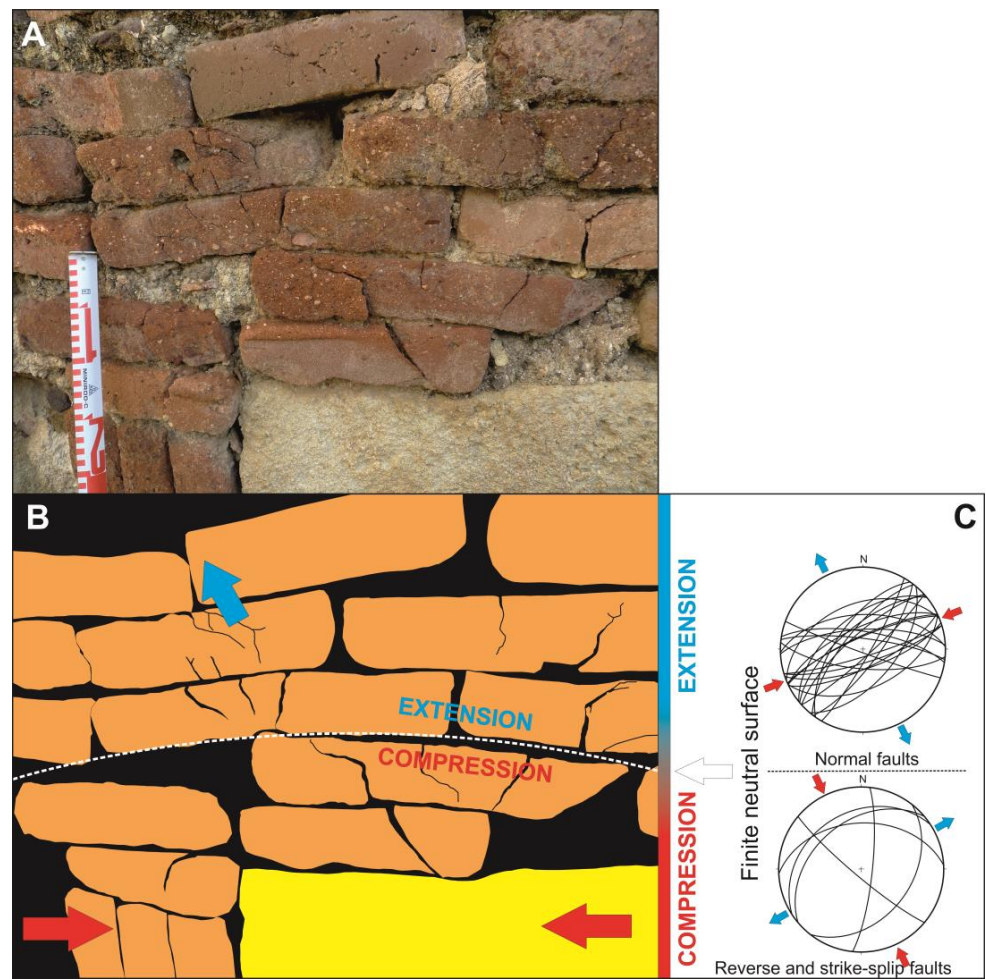


Figure 12. Deformed brick-made walls in the corridor of the Alberca House: (A) Fractures in bricks-made walls; (B) interpretative sketch of the deformation structures in bricks (orange) and masonry block (yellow); the red arrows represent the maximum horizontal strain, and the dashed line is the finite neutral surface; (C) stereonet of reverse and strike-slip faults generated under the finite neutral surface (compression) and normal faults over the finite neutral surface (extension).

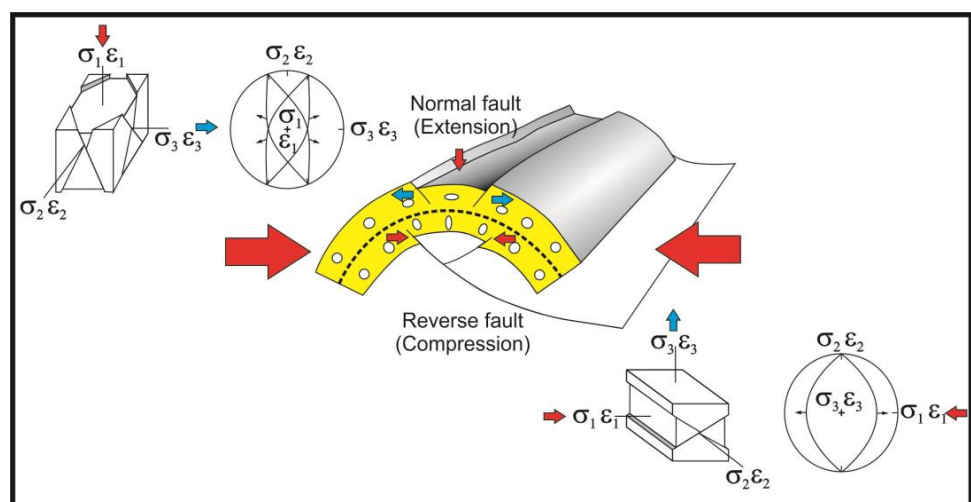


Figure 13. Structural sketch of brittle deformation generated in a fold. This interpretation is used for the explanation of the conjugated fractures in brick-made walls. Red arrows represent compression and blue ones extension; the dashed line is the finite neutral surface.

6.6. Conjugated Fractures on Regular Pavements (XFP)

Pavements constitute a sensible structure under a strain field, and it can be deformed both by brittle and ductile process [55]. Any construction element with a fragile behavior can contain fractures generated by seismic oscillatory movements. Examples of ground shaking deformations are shocks and oriented fracturing in pavement flagstones as described in the archaeological site of the ancient Roman city of *Baelo Claudia* (Spain) [40,56]. Pavements formed by regular marble flagstones from Medina Azahara are a good example of this type of deformation. Plundering suffered during centuries in Medina Azahara have luckily preferred the larger and better-preserved marble flagstones or tiles, not paying attention to the broken ones, otherwise most interesting elements for archaeoseismological research. These broken marble flagstones are those observed today at the archaeological site and that have been reconstructed during the archaeological works.

The two most interesting areas are the Abderraman III Saloon (Figures 4 and 14) and its attached rooms (Figures 4 and 15). A total of 24 fractures (12 pairs of conjugated fractures) have been measured within the Abderraman III Saloon (Figure 14C). The direction of maximum horizontal shortening is in the bisector of the acute angle formed by the conjugated fracture systems, which in this case is in a N156° E direction. In the sector of the Attached Rooms, 16 fractures (8 pairs of conjugated fractures) were measured, obtaining a similar result that in the previous site, with an average direction of maximum horizontal shortening of N164° E (Figure 15C).

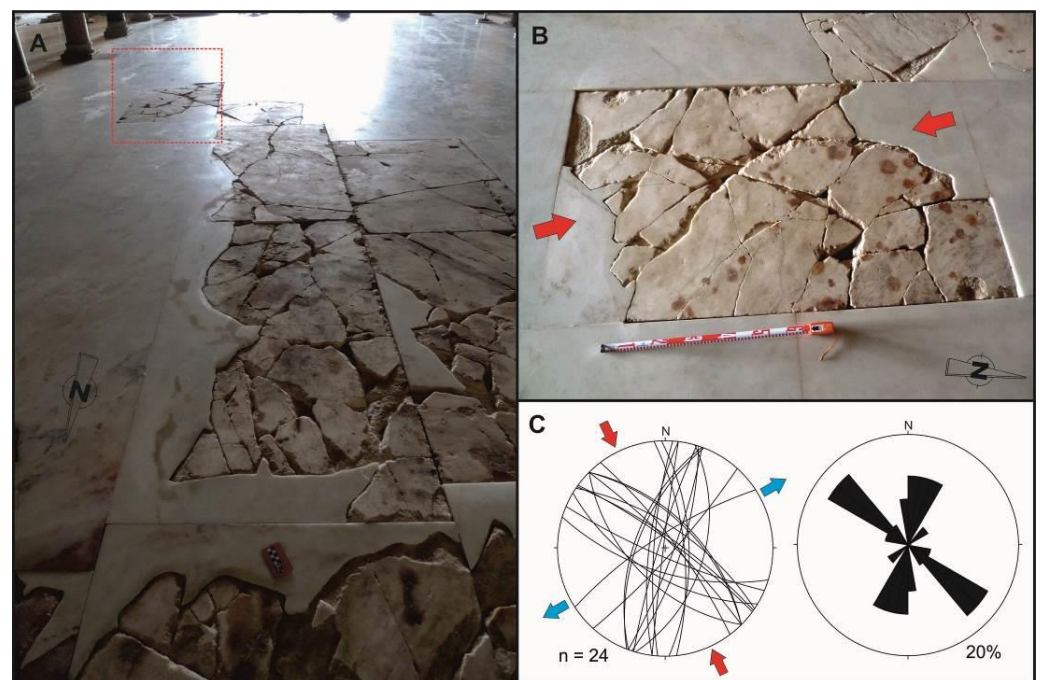


Figure 14. Conjugated fractures in the in the Abderraman III Saloon: (A) reconstructed original marble flagstone; (B) close view of a marble flagstone with conjugated fractures (marked with a red dashed line in (A)); (C) stereonet and rose diagram of conjugated fractures (red arrows: compression; blue arrows: extension).

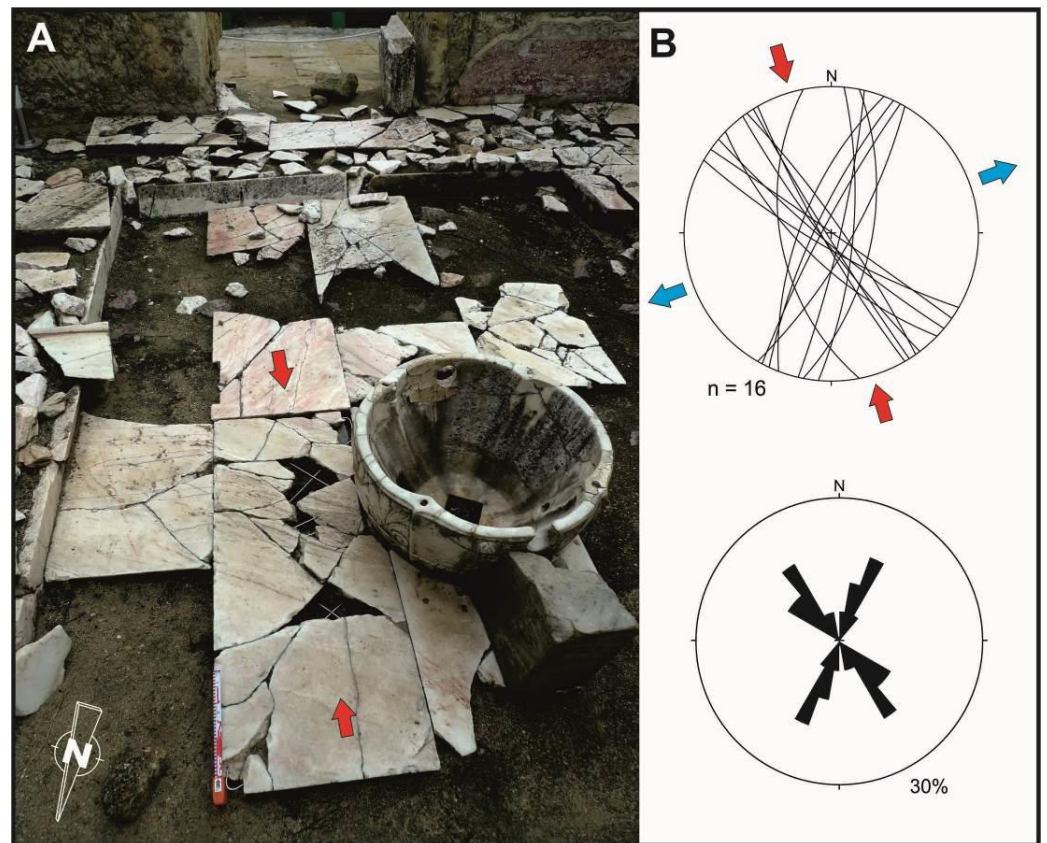


Figure 15. Conjugated fractures in the in the Attached Rooms to the Abderraman III Saloon: (A) reconstructed original marble flagstones; (B) stereonet and rose diagram of conjugated fractures (red arrows: compression; blue arrows: extension).

6.7. Folds on Regular Pavements (FPV)

The surface seismic waves can produce a permanent deformation of the ground, generating folds in the ground surface [40,41,43,44,49,56]. When the affected surfaces are paved, the seismic deformation can generate folds in these pavements, with the direction of maximum horizontal shortening (SHmax) perpendicular to the fold axes [44,45]. The affected flagstones behave as flat elements that adapt to the folding of the underlying ground. Therefore, measuring the orientation of individual flagstones and plotting polar diagrams (Figure 16) we obtain the plane containing the aforementioned SHmax direction.

This classical geological method to characterize the folds has been used in the folded pavement of the Mosque (Figures 4 and 16A) to obtain the SHmax orientation from the deformed pavement. The floor of the mosque, consisting of terracotta tiles (80 cm × 90 cm), shows folds with a wavelength of 1.5–2.3 m. The orientation of the tiles was determined measuring perpendicular sections to the fold axes and obtaining average orientations of the direction of the plane containing the poles of these planes, in this case with an orientation N125° E (Figure 16B,C).

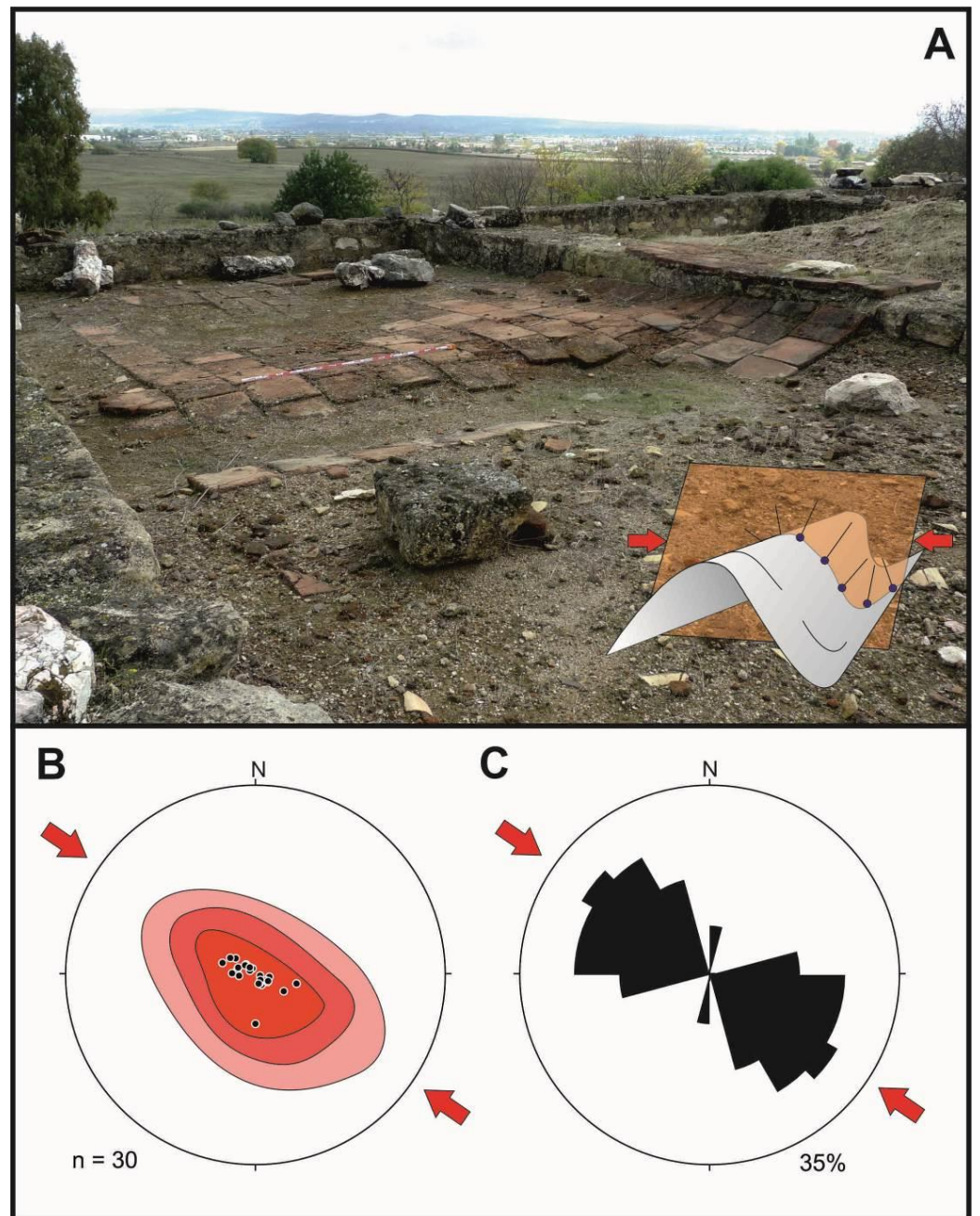


Figure 16. (A) Folds in terracotta regular pavement in the mosque; (B) density diagram of pole representation of flagstones; (C) rose diagram of the poles of the flagstones. Red arrows represent the maximum horizontal strain.

In addition to folds, the floor of the mosque shows differential compaction of the ground. The Mosque was built on the same hillside (slope) as the rest of the city, so half the floor of the building had to be terraced and the other half rests on the infilling extracted from the terracing, being this artificial filling where the main compaction phenomena occur. As a present-day example, during the 2011 Lorca earthquake (Spain), differential compaction triggering pavement deformations was documented in anthropic fillings [49]. The cyclic shear movements generated by the Lorca earthquake caused the internal reorganization of the particles of the artificial fillings inducing an increase of packing and a decrease of porosity, inducing differential compaction and folding of the overlaying elements of the pavement. A similar phenomenon has been observed in Medina Azahara Mosque, where the vertical compaction of the ground surface reaches more than 30 cm (Figures 16 and 17). Therefore, in this case, in addition to the horizontal deformation, a complementary vertical deformation took place because of differential compaction of the ground. The sum of both deformations produced a fold interference figure with a “egg box” pattern, known in structural geology as Type 1 interference structure [57]. This phenomenon can be observed at the SE end of the northernmost nave of the Mosque (Figure 17A), where the two dominant directions of folding are N034° E and N125° E (Figure 17B,C), the first one related to the seismic wave deformation (which would be perpendicular to it, N124° E) and the second one to the effects of ground compaction.

6.8. *Dipping Broken Corners in Columns (DBC)*

As already mentioned in the section on deformed vaults (6.3: DDV), architectural structures with a circular base have no previous anisotropies that condition their movement when facing seismic waves. This is the case of the columns that can move and oscillate freely around the 360° of their supporting base. The same happens with the bases, drums and shafts of these columns, which are also circular in shape section [1,2]. The oscillation movements produced by the seismic waves induce an alternating increase of load in the direction of seismic waves arrival (and opposite) leading to the cracking and splitting at the drum joints; these structures are called dipping broken corners [40,41,44,48]. This increase of the load in a punctual way can produce the fracturing of the drum at its base. The fracture plane will be perpendicular to the direction of oscillation produced by the earthquake, so the poles of these fracture planes can be used to determine the direction of oscillation.

The building that presents the best examples of columns with circular section is the Abderraman III Saloon (Figure 4). The reception hall of the lounge has a set of 24 marble columns, 12 of which display fractures at the edge of their bases (Figure 18). Only the original bases were used to take measures, as some of them have been replaced by new drums during the restoration works. The average orientation of the poles of the fracture planes is N145° E, and the measurements are very homogeneous (Figure 18A). Another fractured base has been identified around the attached rooms to the saloon (Figure 18B).

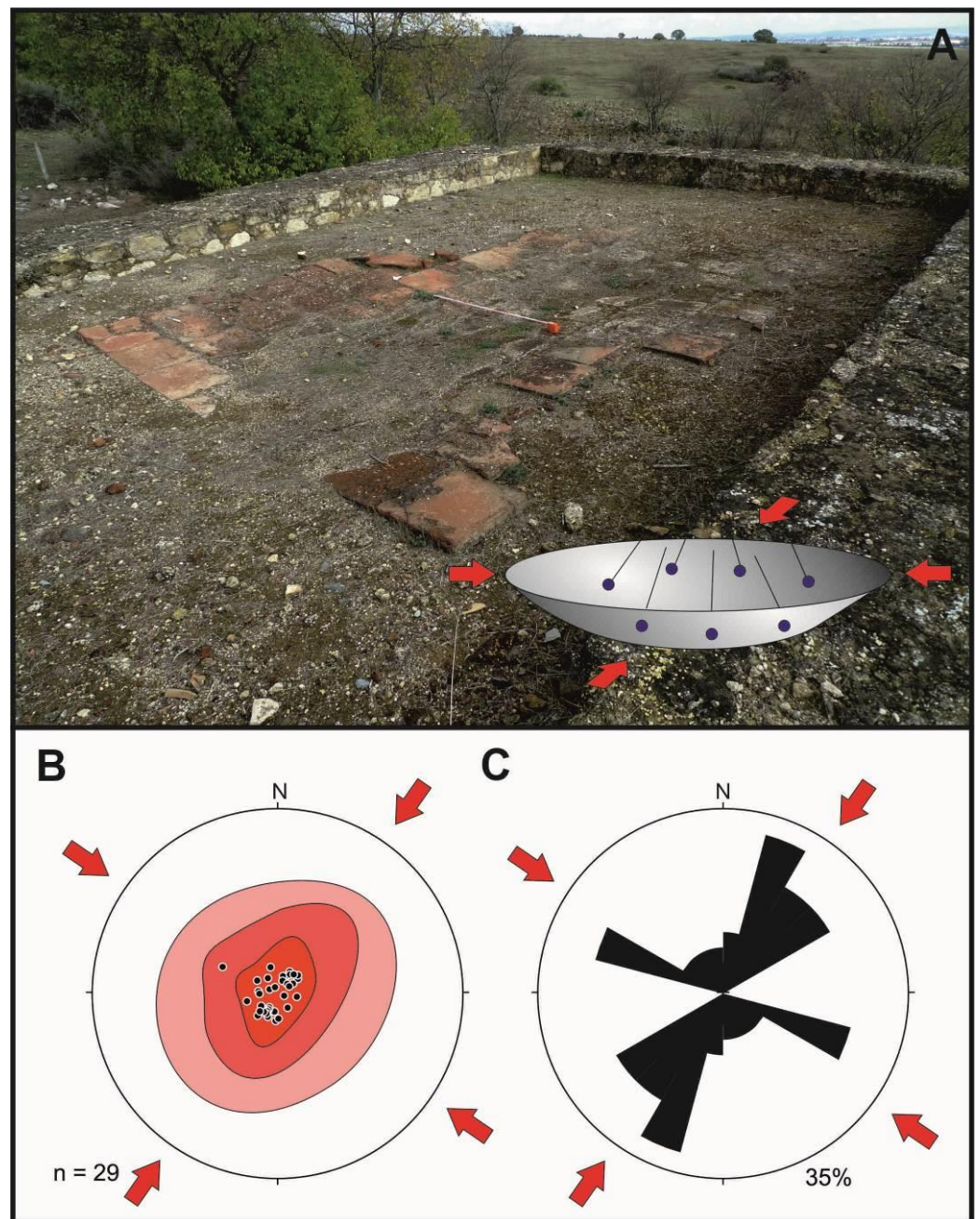


Figure 17. (A) Interference of folds in terracotta regular pavement in the Mosque, the fold has an interference figure Type 1 (egg box pattern); (B) density diagram of measured flagstone poles; (C) rose diagram of the deformed flagstone poles. Red arrows represent the maximum horizontal strain (SHmax).

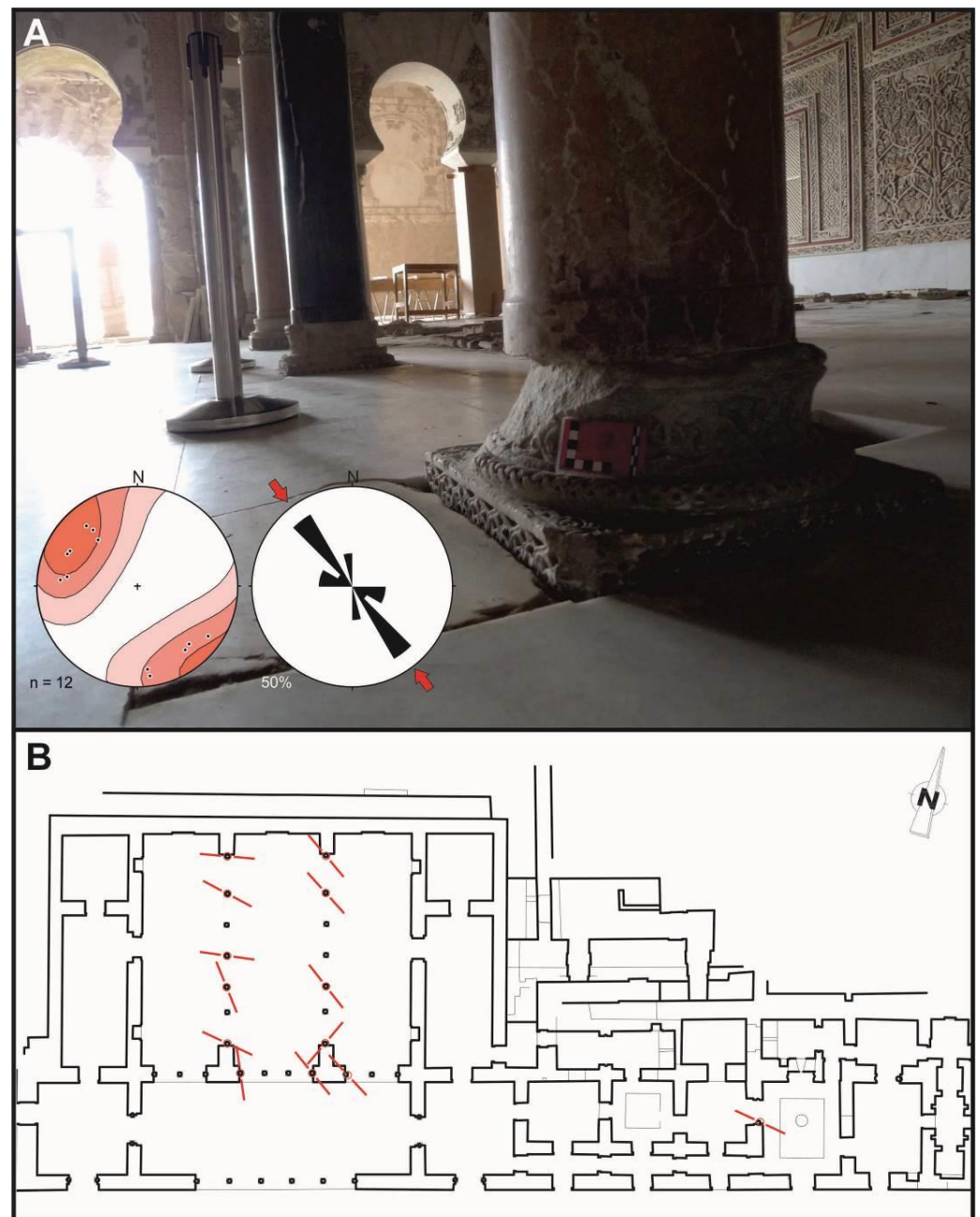


Figure 18. Dipping broken corners in the base of columns in the Abderraman III Saloon; (A) Close up view of a dipping broken corner in the base of a column and density and rose diagram of the poles of the fractures; (B) Map of the Abderraman III Saloon and Attached Rooms (red lines is the horizontal projection of the dipping broken corners poles).

7. Discussion and Conclusions

The classification and analysis of the studied deformation structures by means of geological structural analysis provide an overall view of the structural arrangement of damage across the entire archaeological site. The study comprehends a total of 163 structural measurements on the orientation and direction (when possible) of deformation structures, pointing to a consistent $N145^{\circ}\text{--}150^{\circ}\text{ E}$ average orientation of damage (Figure 19). This result has been obtained from the analysis of eleven different types of deformation structures catalogued as “Earthquake Archaeological Effects” (EAEs) [41,45], and worldwide recognized as indicators of ancient earthquakes, e.g., [40,48,50,53,55,58–60].

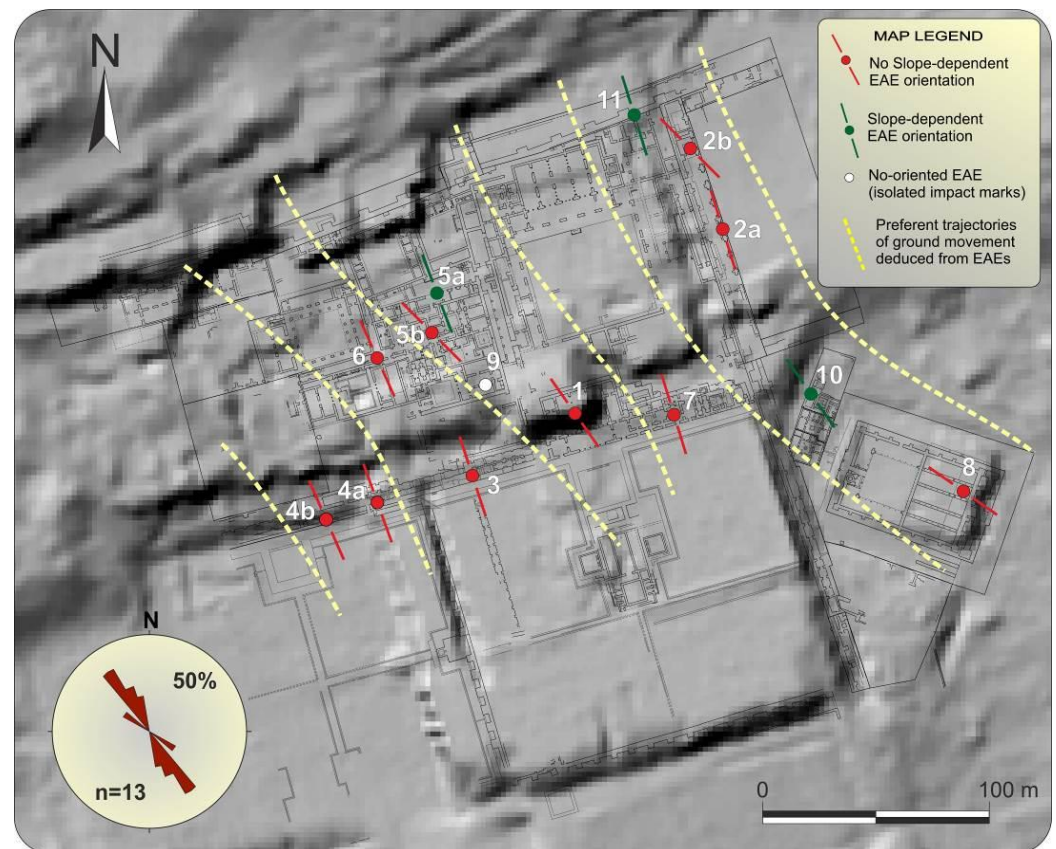


Figure 19. Map of the Caliphal City of Medina Azahara showing the average trajectories of maximum horizontal strain (yellow dashed lines) obtained from the geological structural analysis of EAEs. Number codes refer to surveyed sites referenced in Figure 4 (Section 5). The urban map of the archaeological site is showed on the Digital Terrain Model (2 m/pixel) obtained from Lidar data of the PNOA database (IGN): <https://pnoa.ign.es/el-proyecto-pnoa-lidar> (accessed on 20 February 2022).

Some of the analyzed EAEs are subparallel to the overall ground slope of the site (Figure 19) so they could be attributed to directional collapses by slope process before or during the earlier burial stages of the abandoned city (i.e., some tilted and wall collapses; Figures 11 and 19). Other EAEs can only be related to building-oriented damage (BOD) of seismic origin. This is the case of dropped or displaced keystones (Figures 6–8), rotation of structural elements (Figure 10), conjugated fractures in pavements (Figures 14 and 15), folded pavements (Figures 16 and 17), impact marks in clean pavements (Figure 9) and dipping broken corners in the base of columns in the Abderraman III Saloon (Figure 18). Some of the modern archaeological excavations indicate that the site was early buried after its abandonment. In the houses attached to the mosque (sector 10 in Figure 4) there are collapsed walls and roofs that directly impacted on the old pavement, with piles of ceiling tiles oriented in a NW–SE direction coming from the south, i.e., counter-slope collapses [37]. This author indicates that this destruction horizon contains dark clayey levels with animal bones and pottery fragments of a clear caliphal chronology (≤ 1009 CE) which was rapidly buried by a thick pile of debris-slope deposits incorporating many elements, blocks and pottery fragments of the ruined city. These upper debris levels contain Hispano-Muslim rounded pottery fragments of post-caliphal age, sandy levels as well as rubble and stucco horizons from the medieval plundering of the ruins [37].

This fragmentary information from punctual modern excavations does not demonstrate the seismic nature of the studied deformations, but reinforces the hypothesis on their seismic origin suggested by the analysis of oriented damage developed in this paper. That is, the homogeneous direction of ground motion deduced from the performed analysis

(Figure 19) indicates that the oriented damage recorded in Medina Azahara can be certainly related with a damaging earthquake (\geq VII MSK) that contributed to the destruction and ruin of the city. Similar oriented patterns have been observed during recent instrumental earthquakes being possible to relate them to the primary arrival direction of surface seismic waves and earthquake source parameters [43,46,47].

Moderate earthquakes occurred between 971 and 974 CE (Appendix A) and were local events affecting the city of Córdoba [9,10], but they can hardly be correlated with the observed damage. These events occurred during the last years of use of Medina Azahara as Caliphal residence, just before its relocation in Medina al-Zahira in the year 981 CE [36]. The 974 CE event was the only one energetic enough to damage the city as it affected the city of Córdoba and its surroundings, being felt in the whole Al-Andalus at such distant villages as Coria in Extremadura [9] about 300 km NW of Córdoba. Critical reviews on historical seismicity in Spain by [10], suggests that this is the unique event of this period that can be certainly located in Cordoba. The following 986–987 CE earthquake occurred during the early abandonment of Medina Azahara and it was described as strong enough to damage one of the bridges at Cordoba. However, this event is only documented in a work [33] and it is a doubtful earthquake not catalogued in the historical database of IGN and IAG.

The AD 1024–1025 earthquake is considered “the Great Earthquake of al-Andalus” and it is listed in the IGN and IAG seismic catalogues with an intensity X MSK [8,14,15]. More recently, this earthquake is considered to have an intensity VIII-IX EMS (European Macroseismic Scale), with an estimated magnitude > 5.5 Mw [61] (Appendix A). This earthquake is documented in Arabic sources and its description includes collapse of mountains, violent ground movement and destruction of buildings [32,62]. The fact that this event occurred under confusing socio-political circumstances during the “*fitna*” (1009–1031 CE) may be the reason why it was overlooked by the local historians of Cordoba, resulting in its poor documentation. Of special significance is the fact that the Caliphal city was moved from Medina Azahara during 980–981 CE. Therefore, the 1024–1025 event occurred in an early abandonment stage of the city soon after its plundering by the Berber troops in 1010 CE (Figure 3). All these factors could conjugate to produce most of the oriented damage analyzed in this paper and contribute to the early ruin of the site. As suggested by modern archaeological excavations, the ruin levels correspond to the caliphal period which truly finished in 1031 CE (Figure 3). This ruinous state led to the use of this ancient city as a quarry for centuries, removing much of the archaeological evidence of earthquakes (EAEs). However, the remaining EAEs indicate a probable seismic origin, apparently produced by a unique event given the consistent oriented damage (N145°–150° E; Figure 19). In this sense, the 1169–1170 CE Andujar earthquake (X MSK) induced important damage and fatalities in the city of Cordoba (\geq VII MSK), as reported by contemporaneous Arabic accounts (see Section 3), so it can be considered as another probable damaging event for the site.

Regarding the preserved remains, the probable seismically induced destruction of rich buildings (i.e., Abderramman III Saloon; Figure 18) may have allowed the preservation of many of their luxurious decorative architectural elements (cooper, marbles, etc.) under the rubble, saving them from early robbery and centuries of plundering. Otherwise, these valuable elements would have been stolen, miss-sold and reused in former medieval buildings in Cordoba, the Islamic Iberia, or the entire Maghreb [63]. Collapse levels by earthquake damage would facilitate the preservation of valuable elements under the ruins of the historical heritage from the ancient Al-Andalus, allowing their recovery by the archaeological excavations carried out in Medina Azahara from the early 20th century [5].

In relation to the seismic source of the earthquake, the present available data does not allow us to identify any causative tectonic structure in the zone. However, recent data on the flexural processes along the contact between the Paleozoic substratum of Sierra Morena and the Cenozoic Guadalquivir basin strongly suggest that they must be responsible of the recent seismicity along this important crustal boundary [17,18,25]. In addition, recent geomorphological studies reveal the tectonic rejuvenation of the relief on the northern

edge of the Guadalquivir basin, justifying this rejuvenation by the possible seismic activity of this fault [22]. In fact, the strong earthquakes (\geq IX MSK) that occurred in the zone (Appendix A) have been linked to the backbulge collapse (normal faulting) of the isostatic forebulge of the Betic cordillera in the area [17,18,21,22]. As illustrated in Figure 2, the studied archaeological site is just located upon this complex flexural boundary, historically addressed as the “Guadalquivir Fault”. In fact, the trajectories of average horizontal ground movement (SHmax) displayed in Figure 19 suggests a source occurring WNW of the site, close to the northern margin of the Guadalquivir basin, as the macroseismic epicenter of the 1169–1170 CE event (Figure 1).

At this point, it is just to highlight that the Iberian Peninsula is subject to small convergence rates of 2–3 mm/yr. Accordingly, stronger historical earthquakes had estimated magnitudes of 6.5–7.0 Mw and they are commonly no-surface faulting events [13]. Therefore, the identification of seismic sources for earthquakes occurred around the limit of the first Millennia CE still needs complementary historical and geological data, as well as more modern approaches considering geophysical and remote sensing analyses focused on tectonic geomorphology [64].

Author Contributions: Field research for data record: M.Á.R.-P., M.Á.P., P.G.S., J.L.G.-R., T.B. and J.É. This includes the archaeoseismological compilation, and structural analysis. Archaeological and historical data: A.J.M.C. and P.G.S. Contextualization and bibliographic compilation: M.Á.P., A.J.M.C., P.G.S. and E.R. Mapping and DEMs: Y.S.-S., J.É. and P.G.S. Conceptualization and Modelling: M.Á.R.-P., P.G.S. and M.Á.P. The final model was approved by all the authors, and the manuscript and figures as well. Manuscript redaction: M.Á.R.-P., P.G.S., A.J.M.C., M.Á.P. and T.B. Figures: M.Á.R.-P., P.G.S., Y.S.-S. and M.Á.P. All authors have read and agreed to the published version of the manuscript.

Funding: This research is part of the Spanish Research Project I+D+i PID2021-123510OB-I00 (QTECIBERIA-USAL) funded by the MICIN AEI/10.13039/501100011033/. This is contribution of the QTECT-AEQUA Working Group.

Data Availability Statement: The data set of the EAEs can be downloaded at: Rodríguez-Pascua, M.A., Perucha, M.A., Montejo, A.J., Silva, P.G., Giner-Robles, J.L., Élez, J., Bardají, T., and Roquero, E.: Archaeoseismological evidence of the Medina Azahara destruction in the early 11th century (Córdoba, Spain), Zenodo [data set], <https://doi.org/10.5281/zenodo.5126886> (accessed on 13 October 2022), 2021.

Acknowledgments: We thank all the staff of the Archaeological Site of Medina Azahara (Andalusian Government) for their kind and strong support during the fieldwork. We are especially grateful to Silvia Carmona, Inmaculada Muñoz and Alejandra del Pino. It is a contribution of the Spanish W. G. QTECT-AEQUA.

Conflicts of Interest: The authors declare no conflict of interest.

Appendix A

Table A1. Earthquakes in the region of Cordoba from the 10th to 12th Century. References: IAG (online catalogue Instituto Andaluz de Geofísica) [14]; IGN (Catalogue of Historical Earthquakes, Instituto Geográfico Nacional [15]); PO&TH 80 [8]; MOL 83 [33]; BG&EM 96 [9]; BET 10 [61]; TH 11 [32]; SIL 13 [21]; UD 15 [10].

Date	I Max (MSK)	Estimated Magnitude	Macroseismic Epicentre	Affected Zone	Agency or Main Reference
881 26 May	X MSK	7.2 Mw	Gulf of Cádiz	Al-Andalus Great Earthquake–Tsunami event	IAG, IGN, PO&TH 80, BG&EM 96, TH 11, UD 15
944 3 July	VII MSK		Córdoba <i>s.l.</i>	Córdoba	IAG, IGN, PO&TH 80, UD15
955 29 August	VII MSK	5.7 Mw	Córdoba <i>s.l.</i>	Córdoba. Moderate earthquake with aftershock	IAG, IGN, PO&TH 80, BG&EM 96, UD 15

Table A1. Cont.

Date	I Max (MSK)	Estimated Magnitude	Macroseismic Epicentre	Affected Zone	Agency or Main Reference
957			Gulf of Cádiz	Córdoba zone.	IAG, IGN, BG&EM 96, UD15
971 19 December			Córdoba s.l.	Córdoba city	IAG, IGN, BG&EM 96, UD15
973 20 May			Córdoba s.l.	Córdoba city	IAG, IGN, BG&EM 96, UD15
974 9 November			Córdoba s.l.	Córdoba city and Western Al-Andalus	IAG, IGN, BG&EM 96, TH 11, UD15
986–987			Córdoba s.l.	Córdoba. Moderate damage	MOL 83
1024 15 March	X MSK	>5.5 Mw	Al-Andalus	Al-Andalus Great Earthquake event	IAG, IGN, PO&TH 80, BG&EM 96, TH 11, BET 10
1079			Gulf of Cádiz	Eastern Al-Andalus	IAG, IGN, PO&TH 80, BG&EM 96, TH 11
1069	IX MSK VIII-IX EMS	6.0 Mw	Andujar	Guadalquivir valley: felt and damage also in Sevilla and Córdoba	IAG, IGN, PO&TH 80, BG&EM 96, BET 10, TH 11
No relevant earthquakes in the zone until 1504 CE					
1504 5 April	X MSK VIII-IX EMS	6.7 Mw	Carmona	Guadalquivir Valley Felt in Córdoba	IAG, IGN, PO&TH 80, BET 10, SIL 13

References

- Ambraseys, N.N. Earthquakes and archaeology. *J. Archaeol. Sci.* **2006**, *33*, 1008–1016. [CrossRef]
- Stiros, S.C. Identification of Earthquakes from Archaeological Data: Methodology, Criteria and Limitations. In *Archaeoseismology*; Stiros, S., Jones, R., Eds.; Fitch Laboratory Occasional Paper 7; British School at Athens: Athens, Greece, 1996; pp. 129–152.
- Galadini, F.; Hinzen, K.G.; Stiros, S. Archaeoseismology: Methodological issues and procedure. *J. Seismol.* **2006**, *10*, 395–414. [CrossRef]
- Maíllo Salgado, F. *La Caída del Califato de Córdoba y los Reyes de Taifas (al-Bayan al-Mugrit)*; Universidad de Salamanca: Salamanca, Spain, 1993; 263p.
- Vallejo Triano, A. *Madinat Al-Zahra. Official Guide to the Archaeological Complex. Conjuntos Arqueológicos y Monumentales*; Guías Oficiales. Consejería de Cultura, Junta de Andalucía: Andalucía, Spain, 2009; p. 182.
- Bariani, L. *Almanzor*; Nerea: San Sebastián, Spain, 2003; p. 298.
- García Gómez, E. *El Califato de Córdoba el “Muqtabis” de Ibn Hayyan. Anales Palatinos del Califa de Córdoba al-Hakam II, por Isa ibn Ahmad al-Razi (360–364 H. = 971–975 J.C.)*; Translation of an Arabic Manuscript of the Real Academia de la Historia by Emilio García Gómez; Sociedad de Estudios y Publicaciones: Madrid, Spain, 1967; p. 281.
- Poirier, J.P.; Taher, M.A. Historical Seismicity in the Near and Middle East, North Africa and Spain from Arabic Documents, (7th–13th Century). *Bull. Seism. Soc. Am.* **1980**, *70*, 2185–2201. [CrossRef]
- Bretón González, M.; Espinar Moreno, M. *Fenómenos Sísmicos Que Afectaron a las Tierras Andaluzas en los Siglos IX al XII Según las Crónicas Musulmanas*; Homenaje en Honor al Profesor Fernando de Miguel Martínez; Universidad de Granada: Granada, Spain, 1996; pp. 47–76.
- Martínez-Solares, J.M.; Mezcuá, J. *Catálogo Sísmico de la Península Ibérica (880 A.C.–1900)*; Instituto Geográfico Nacional. Ministerio de Fomento: Madrid, Spain, 2002; p. 756.
- Udías, A. Historical Earthquakes (before 1755) of the Iberian Peninsula in Early Catalogs. *Seism. Res. Lett.* **2015**, *86*, 999–1005. [CrossRef]
- González, A. The Spanish National Earthquake Catalogue: Evolution, precision and completeness. *J. Seismol.* **2017**, *21*, 435–471. [CrossRef]
- Silva, P.G.; Rodríguez-Pascua, M.A.; Giner-Robles, J.L.; Pérez-López, R.E.; García-Tortosa, F.J.; Gómez Vicente, P.; Bardají, T.; Perucha, M.A.; Huerta, P.; Lario, J.J. *Catálogo de los Efectos Geológicos de los Terremotos de España*, 2nd ed.; Revisada y Ampliada; Riesgos Geológicos y Geotecnia 6; IGME: Madrid, Spain, 2019; p. 804.
- IAG. *Catálogo de Terremotos Históricos de Andalucía Online*; Instituto Andaluz de Geofísica: Granada, Spain, 2021. Available online: http://iagpds.ugr.es/pages/informacion_divulgacion/terremotos_historicos (accessed on 12 October 2022).
- IGN. *Actualización de Mapas de Peligrosidad Sísmica de España 2012*; Ministerio de Fomento; Instituto Geográfico Nacional: Madrid, Spain, 2013; p. 267.
- González-Delgado, J.A.; Civis, J.; Dabrio, C.J.; Goy, J.L.; Ledesma, S.; Sierro, F.J.; Zazo, C. Cuenca del Guadalquivir. In *Geología de España*; Vera, J.A., Ed.; SGE-IGME: Madrid, Spain, 2004; pp. 543–550.
- García-Castellanos, D.; Fernández, M.; Torné, M. Modelling the evolution of the Guadalquivir foreland basin southern Spain. *Tectonics* **2002**, *21*, 1018. [CrossRef]

18. Marín-Lechado, C.; Pedrera, A.; Peláez, J.A.; Ruiz-Constán, A.; González-Ramón, A.; Henares, J. Deformation style and controlling geodynamic processes at the eastern Guadalquivir foreland basin (Southern Spain). *Tectonics* **2017**, *36*, 1072–1089. [[CrossRef](#)]
19. Hernández Pacheco, E. Historia Geológica del Guadalquivir. *Boletín Real Acad. Cienc. Córdoba* **1944**, *51*, 6–49.
20. Hernando Luna, R. Estudio sobre “la Gran Falla Bética” del borde meridional del Macizo Ibérico. *Boletín Real Acad. Cienc. Córdoba* **2000**, *79*, 61–64.
21. Silva, P.G.; Rodríguez Pascua, M.A.; Pérez López, R.; Giner Robles, J.; Lario, J.; Bardají, T.; Goy, J.L.; Zazo, C. Geological and Archaeological effects of the AD 1504 Carmona Earthquake (Guadalquivir valley, South Spain): Preliminary data on probable seismic sources. *Cuatern. Geomorfol.* **2013**, *27*, 9–32.
22. Expósito, I.; Jiménez-Bonilla, A.; Delchiaro, M.; Yanes, J.L.; Balanyá, J.C.; Moral-Martos, F.; Della Seta, M. Geomorphic signature of segmented relief rejuvenation in the Sierra Morena, Betic forebulge, Spain. *Earth Surf. Dynam.* **2022**, *10*, 1017–1039. [[CrossRef](#)]
23. Goy, J.L.; Zazo, C.; Rodríguez-Vidal, J. Cordilleras Béticas—Islas Baleares. In *Geomorfología de España*; Gutiérrez-Elorxa, M., Ed.; Rueda: Madrid, Spain, 1994; pp. 123–157.
24. De Vicente, G.; Vegas, R.; Guimerá, J.; Cloetingh, S. Estructura alpina del Antepaís Ibérico. In *Geología de España*; Vera, J.A., Ed.; SGE-IGME: Madrid, Spain, 2004; pp. 587–633.
25. Morales, J.; Azañón, J.M.; Stich, D.; Roldán, F.J.; Pérez-Peña, J.V.; Martín, R.; Cantavella, J.V.; Martín, J.B.; Mancilla, F.; González-Ramón, A. The 2012–2013 earthquake swarm in the eastern Guadalquivir basin (South Spain): A case of heterogeneous faulting due to oroclinal bending. *Gond. Res.* **2015**, *28*, 1566–1578. [[CrossRef](#)]
26. Serrano, I.; Torcal, F.; Martín, J.B. High resolution seismic imaging of an active fault in the eastern Guadalquivir Basin (Betic Cordillera, Southern Spain). *Tectonophysics* **2015**, *660*, 79–91. [[CrossRef](#)]
27. Peláez, J.A.; Castillo, J.C.; Sánchez Gómez, M.; Martínez Solares, J.M.; López Casado, C. Fuentes medievales y posibles evidencias arqueológicas del terremoto de Andújar de 1170. *Boletín Inst. Estud. Gienenses* **2005**, *192*, 139–177.
28. Castelló Montori, R.; Ramírez Copeiro, J. *Mapa Geológico y Memoria de la Hoja n° 922 (Santa María de Trassierra)*; Mapa Geológico de España E. 1:50,000, 2nd Serie (MAGNA); IGME: Madrid, Spain, 1975; p. 46.
29. Quesada, C.; Fonseca, P.E.; Munhá, J.; Oliveira, J.T.; Ribeiro, A. The Beja-Acebuches Ophiolite (Southern Iberia Variscan Fold Belt). Geological characterization and geodynamic significance. *Bol. Geol. Min.* **1994**, *105*, 3–49.
30. Sánchez García, M.T.; Bellido, F.; Quesada, C. Geodynamic setting and geochemical signatures of Cambrian-Ordovician rift-related igneous rocks (Ossa-Morena Zone, SW Iberia). *Tectonophysics* **2003**, *365*, 233–255. [[CrossRef](#)]
31. Barrios-Neira, J.; Montealegre, L.; Nieto, M.; Palma, J. Contribución al estudio litológico de los materiales empleados en monumentos de Córdoba de distintas épocas. *Arqueol. Arq. Mit.* **2003**, *2*, 47–53. [[CrossRef](#)]
32. Taher, M.A. *Nussus (Textos Árabes): Terremotos y Volcanes en el Mundo Árabe Desde el Comienzo de la Historia Islámica Hasta el Siglo XII. La Hégira: Del siglo VI a lo Precioso, Ashar Al-Mulladin*; General Egyptian Book Organization: El Cairo, Egypt, 2011; p. 10.
33. Molina, L. *Una Descripción Anónima de al-Andalus*; Edited and Translated with Introduction, Notes and Indexes, by Luis Molina Vol II. Consejo Superior de Investigaciones Científicas; Instituto “Miguel Asín”: Madrid, Spain, 1983; pp. 105–107.
34. Espinar Moreno, M. *Trabajos Sobre Sismicidad Histórica en Andalucía II*; Libros de Estudios sobre Patrimonio, Cultura y Ciencia Medievales (EPCCM); Universidad de Granada—Instituto Andaluz de Geofísica y Desastres Naturales: Granada, Spain, 2021; p. 276.
35. Akasoy, A. Islamic Attitudes to Disasters in the Middle Ages: A Comparison of Earthquakes and Piagues. *Mediev. Hist. J.* **2007**, *10*, 387–410. [[CrossRef](#)]
36. Martínez Núñez, M.A. Recientes hallazgos epigráficos en Madinat al-Zahra y nueva onomástica relacionada con la dar al-sina califal. *Anejos Arqueol. Territ. Mediev.* **2015**, *1*, 74.
37. Cano Montero, J.I. Resultados preliminares de la intervención arqueológica puntual en un sector del muro norte de las viviendas fronterizas a la Mezquita Aljama de Madinat al-Zahra. *Cuad. Madinat Zahar.* **2008**, *6*, 275–302.
38. Kamai, R.; Hatzor, Y.H. Numerical analysis of block displacements in ancient masonry structures: A new method to estimate historic ground motions. *Int. J. Numer. Anal. Methods Geomech.* **2007**, *32*, 1321–1340. [[CrossRef](#)]
39. Korjenkov, A.M.; Tabaldiev, S.; Bobrovskii, A.V.; Bobrovskii, A.V.; Mamyrov, E.M.; Orlova, L.A. A macroseismic study of the Taldy-Sai caravanserai in the Kara-Bura River valley (Talas basin, Kyrgyzstan). *Russ. Geol. Geophys.* **2009**, *50*, 63–69. [[CrossRef](#)]
40. Silva, P.G.; Reicherter, K.; Grützner, C.; Bardají, T.; Lario, J.; Goy, J.L.; Zazo, C.; Becker-Heidmann, P. Surface and subsurface palaeoseismic records at the ancient Roman city of Baelo Claudia and the Bolonia Bay area, Cádiz (south Spain). In *Palaeoseismology. Historical and Prehistorical Records of Earthquake Ground Effects for Seismic Hazard Assessment*; Reicherter, K., Michetti, M., Silva, P.G., Eds.; Geological Society of London, Special Publication: London, UK, 2009; Volume 316, pp. 93–121. [[CrossRef](#)]
41. Rodríguez-Pascua, M.A.; Perez-Lopez, R.; Silva, P.G.; Giner-Robles, J.L.; Garduño-Monroy, V.H.; Reicherter, K. A comprehensive classification of earthquake archaeological effects (EAE) for archaeoseismology. *Quat. Int.* **2011**, *242*, 20–30. [[CrossRef](#)]
42. Giner-Robles, J.L.; Rodríguez-Pascua, M.A.; Pérez-López, R.; Silva, P.G.; Bardají, T.; Grützner, C.; Reicherter, K. *Structural Analysis of Earthquake Archaeological Effects (EAE) Baelo Claudia Examples (Cádiz, South Spain)*; UNED: Madrid, Spain, 2009; 137p.
43. Giner-Robles, J.L.; Pérez-López, R.; Rodríguez-Pascua, M.A.; Silva Barroso, P.G.; Martín-González, F.; Cabañas, L. Oriented Structural analysis of seismically oriented damage caused by the Lorca earthquake of 11 May 2011: Application to archaeoseismology. *Boletín Geológico Min.* **2012**, *123*, 503–513.
44. Giner-Robles, J.L.; Rodríguez-Pascua, M.A.; Silva, P.G.; Pérez-López, R. Efectos sísmicos en yacimientos arqueológicos: Catalogación y cuantificación arqueosismológica. *Boletín Geológico Min.* **2018**, *129*, 451–467. [[CrossRef](#)]

45. Giner-Robles, J.L.; Rodríguez-Pascua, M.A.; Pérez López, R.; Silva, P.G.; Bardají, T.; Roquero, E.; Elez, J.; Perucha, M.A. Geological structural analysis applied to archaeoseismology. In *Handbook of Cultural Heritage Analysis*; D'Amico, S., Venuti, V., Eds.; Springer Nature Switzerland AG: Berlin/Heidelberg, Germany, 2022; pp. 1763–1778. [[CrossRef](#)]
46. Motoki, K.; Seo, K. Strong motion characteristics near the source region of the Hyogoken-Nanbu earthquake from analyses of the directions of structural failures. In *Proceedings of the 12th World Conference on Earthquake Engineering*, Auckland, New Zealand, 30 January–4 February 2000; Paper 959. p. 6.
47. Howard, J.K.; Tracy, C.A.; Burnsa, R.G. Comparing observed and predicted directivity in near-source ground motion. *Earthq. Spectra* **2005**, *21*, 1063–1092. [[CrossRef](#)]
48. Marco, S. Recognition of earthquake-related damage in archaeological sites: Examples from the Dead Sea fault zone. *Tectonophysics* **2008**, *453*, 148–156. [[CrossRef](#)]
49. Rodríguez-Pascua, M.A.; Perez-Lopez, R.; Martín-Gonzalez, F.; Giner-Robles, J.L.; Silva, P.G. Efectos arquitectónicos del terremoto de Lorca del 11 de mayo de 2011. Neoformación y reactivación de efectos en su Patrimonio Cultural. *Bol. Geológico Min.* **2012**, *123*, 487–502.
50. Kázmér, M.; Major, B. Distinguishing damages from two earthquakes: Archaeoseismology of a Crusader castle (Al-Marqab citadel, Syria). *Geol. Soc. Am. Spec. Pap.* **2010**, *471*, 185–198.
51. Korjenkov, A.; Kaiser, D. Historical-macroseismic study of the town church in Wittstock, northern Germany. In *Proceedings of the 11th FIG Symposium on Deformation Measurements*, Santorini, Greece, 25–28 May 2003; p. 4.
52. Vallejo Triano, A.; Escudero Aranda, J. Crónica del Conjunto, años 1992–1997. *Cuad. Madinat Zahar.* **1999**, *4*, 235–296.
53. Karakhanyan, A.; Avagyan, A.; Sourouzian, H. Archaeoseismological studies at the temple of Amenhotep III, Luxor, Egypt. *Geol. Soc. Am. Spec. Pap.* **2010**, *471*, 199–222. [[CrossRef](#)]
54. De Vicente, G. Análisis Poblacional de Fallas: El Sector de Enlace Sistema Central-Cordillera Iberica. Ph.D. Thesis, Public University Complutense de Madrid, Madrid, Spain, 1988; 317p.
55. Altunel, E. Evidence for Damaging Historical Earthquakes at Priene, Western Turkey. *Turk. J. Earth Sci.* **1998**, *7*, 25–35.
56. Silva, P.G.; Borja, F.; Zazo, C.; Goy, J.L.; Bardají, T.; De Luque, L.; Lario, J.; Dabrio, C.J. Archaeoseismic record at the ancient Roman City of Baelo Claudia (Cádiz, south Spain). *Tectonophysics* **2005**, *408*, 129–146. [[CrossRef](#)]
57. Ramsay, J.G.; Huber, M.I. *The Technics of Modern Structural Geology. Vol II Folds and Fractures*; Academic Press: London, UK, 1987; p. 700.
58. Korjenkov, A.M.; Baipakov, C.; Chang, Y.; Peshkov-Savelieva, T. Traces of Ancient Earthquakes in Medieval Cities along the Silk Road, Northern Tien Shan and Dzhungaria. *Turk. J. Earth Sci.* **2003**, *12*, 241–261.
59. Korjenkov, A.M.; Kol'chenko, V.A.; Rott, P.G.; Abdieva, S.V. Strong Mediaeval Earthquake in the Chuy Basin, Kyrgyzstan. *Geotectonics* **2012**, *46*, 303–314. [[CrossRef](#)]
60. Rodríguez-Pascua, M.A.; Benavente-Escobar, C.; Rosell-Guevara, L.; Grützner, C.; Audin, L.; Walker, R.; García, B.; Aguirre, E. Did earthquakes strike Machu Picchu? *J. Seismol.* **2020**, *24*, 883–895. [[CrossRef](#)]
61. Benito, M.B.; Navarro, M.; Vidal, F.; Gaspar-Escribano, J.; García-Rodríguez, M.J.; Martínez-Solares, J.M. A new seismic hazard assessment in the region of Andalusia (Southern Spain). *Bull. Earthq. Eng.* **2010**, *8*, 739–766. [[CrossRef](#)]
62. Guidoboni, E.; Comastri, A. *Catalogue of Earthquakes and Tsunamis in the Mediterranean Area from the 11th to the 15th Century*; Istituto nazionale di geofisica e vulcanología: Rome, Italy, 2005; p. 1037. [[CrossRef](#)]
63. Hernández Giménez, F. *Madinat Zahara: Arquitectura y Decoración*; Patronato de La Alhambra: Granada, Spain, 1985; p. 188.
64. Papanikolaou, I.; Van Balen, R.; Silva, P.G.; Reicherter, K. Geomorphology of active faulting and seismic hazard assessment: New tools and future challenges. *Geomorphology* **2015**, *237*, 1–13. [[CrossRef](#)]

Disclaimer/Publisher's Note: The statements, opinions and data contained in all publications are solely those of the individual author(s) and contributor(s) and not of MDPI and/or the editor(s). MDPI and/or the editor(s) disclaim responsibility for any injury to people or property resulting from any ideas, methods, instructions or products referred to in the content.